





Review

Bioactive Marine Xanthenes: A Review

José X. Soares ^{1,2,†}, Daniela R. P. Loureiro ^{1,2,3,†} , Ana Laura Dias ², Salette Reis ¹ , Madalena M. M. Pinto ^{2,3} 
and Carlos M. M. Afonso ^{2,3,*} 

- ¹ Laboratório Associado para a Química Verde (LAQV), Rede de Química e Tecnologia (REQUIMTE), Department of Chemical Sciences, Faculty of Pharmacy, University of Porto, Rua de Jorge Viterbo Ferreira, 228, 4050-313 Porto, Portugal; jfxsoares@ff.up.pt (J.X.S.); dloureiro@ff.up.pt (D.R.P.L.); shreis@ff.up.pt (S.R.)
- ² Laboratory of Organic and Pharmaceutical Chemistry, Department of Chemical Sciences, Faculty of Pharmacy, University of Porto, Rua de Jorge Viterbo Ferreira, 228, 4050-313 Porto, Portugal; up201903848@ff.up.pt (A.L.D.); madalena@ff.up.pt (M.M.M.P.)
- ³ Interdisciplinary Center of Marine and Environmental Investigation (CIIMAR/CIMAR), Edifício do Terminal de Cruzeiros do Porto de Leixões, Av. General Norton de Matos s/n, 4050-208 Matosinhos, Portugal
- * Correspondence: cafonso@ff.up.pt; Tel.: +351-22-042-8500
- † These authors contributed equally to this work.

Abstract: The marine environment is an important source of specialized metabolites with valuable biological activities. Xanthenes are a relevant chemical class of specialized metabolites found in this environment due to their structural variety and their biological activities. In this work, a comprehensive literature review of marine xanthenes reported up to now was performed. A large number of bioactive xanthone derivatives (169) were identified, and their structures, biological activities, and natural sources were described. To characterize the chemical space occupied by marine-derived xanthenes, molecular descriptors were calculated. For the analysis of the molecular descriptors, the xanthone derivatives were grouped into five structural categories (simple, prenylated, *O*-heterocyclic, complex, and hydroxanthenes) and six biological activities (antitumor, antibacterial, antidiabetic, antifungal, antiviral, and miscellaneous). Moreover, the natural product-likeness and the drug-likeness of marine xanthenes were also assessed. Marine xanthone derivatives are rewarding bioactive compounds and constitute a promising starting point for the design of other novel bioactive molecules.

Keywords: xanthone; marine products; natural products; molecular descriptors; antimicrobial; antitumor; drug-like



Citation: Soares, J.X.; Loureiro, D.R.P.; Dias, A.L.; Reis, S.; Pinto, M.M.M.; Afonso, C.M.M. Bioactive Marine Xanthenes: A Review. *Mar. Drugs* **2022**, *20*, 58. <https://doi.org/10.3390/md20010058>

Academic Editor: Bill J. Baker

Received: 17 December 2021

Accepted: 29 December 2021

Published: 8 January 2022

Publisher's Note: MDPI stays neutral with regard to jurisdictional claims in published maps and institutional affiliations.



Copyright: © 2022 by the authors. Licensee MDPI, Basel, Switzerland. This article is an open access article distributed under the terms and conditions of the Creative Commons Attribution (CC BY) license (<https://creativecommons.org/licenses/by/4.0/>).

1. Introduction

The marine environment occupies more than half of the Earth's surface and harbors the largest pool of biodiversity. Among others, marine microorganisms produce specialized metabolites used mostly in interspecies competition and defense from predators. The harsh conditions found in the sea spurs the development of specific biosynthetic pathways that produce metabolites bearing novel scaffolds, quite different from those found in terrestrial sources [1]. Specialized metabolites were optimized by evolution to establish flawless interactions with biological targets [2]. The sum of these factors makes the marine environment a prolific source of structurally diverse bioactive molecules that have a pharmacological interest [3].

Among the most relevant chemical classes of specialized metabolites isolated from the marine biodiversity, xanthenes are a class of oxygen-heterocycles containing a heterocycle containing a dibenzo γ -pyrone moiety [4–6]. Depending on the nature and position of substituents, xanthone derivatives show a wide variety of biological activities making the xanthone scaffold a “privileged structure” in Medicinal Chemistry with a good potential for the discovery of novel hits, leads, and drugs [7].

The chemical space occupied by a collection of substances is usually mapped by molecular descriptors [8]. Molecular descriptors are generically defined as mathematical

representations of molecular features and embrace a vast collection of molecular, physico-chemical, and topological parameters. Each molecular feature is encoded by at least one molecular descriptor. Size is usually inferred by the molecular weight (MW); flexibility by the number of rotatable bonds; lipophilicity by partition coefficient between octanol and water (Log P); polarity by the topological polar surface area (TPSA); solubility by the logarithm of the solubility measured in mol L⁻¹ (log S); and carbon saturation by the fraction of sp³ carbons (Fsp³). Besides providing a numerical expression for chemical features, molecular descriptors allow tracking the suitable pharmacodynamics and pharmacokinetics properties, i.e., allow pursuing drug-likeness. Sets of rules or filters have been proposed over time in order to predict pharmacokinetic behavior. The most common set is the Lipinski's rule of five [9], but other approaches have been suggested by other authors, namely by Veber [10], Ghose [11], Egan [12], and Gleeson [13]. More recently, Bickerton et al. proposed the quantitative estimate of drug-likeness (QED) based on the calculation of the desirability of eight molecular properties [14]. Due to its usefulness in mapping the drug-likeness territory, this model has also been expanded to natural products (NP), creating the concept of NP-likeness evaluated by a score that allows comparing the chemical space covered by NPs with the one covered by synthetic molecules (SM) [15]. The application of this score helps medicinal chemists design molecules that are inspired by nature and have a higher probability of having a suitable pharmacokinetic behavior [16].

In this work, we review 169 bioactive marine xanthone derivatives and present their structures, biological activities, and marine sources. The chemical space occupied by bioactive marine xanthenes is mapped and framed according to the NP-likeness and drug-likeness concepts.

2. Bioactive Xanthenes Isolated from the Marine Environment

The bibliographic research was conducted using Scopus[®], Web of Science[®], and Google Scholar[®] without any temporal restriction. The keywords used were “marine AND xanthone*”.

In total, 169 xanthenes derivatives were identified, which were sorted into 5 different structural categories (Figure 1). Simple oxygenated xanthenes, bearing substituents such as hydroxyl, carboxyl, and methoxy groups, were classified as “simple” xanthenes. Xanthenes bearing isoprenyl groups were classified as “prenylated” compounds. Xanthenes bearing additional *O*-heterocyclic groups, such a pyran or furan ring, were classified as “*O*-heterocyclic” compounds. Xanthenes bearing *O*-heterocyclic and isoprenyl groups were classified as “*O*-heterocyclic” because they have a higher similarity with this category. Dimeric, pseudo-dimeric (one xanthenic and a hydroxanthone nucleus connected by a C-C bond), and glycosylated xanthenes were loosely classified as “complex”. Dihydro-, tetrahydro-, and hexahydroxanthenes were included in the “hydroxanthone” category (Figure 1).

From the considered 5 different structural types, “simple” (28.7%) and “complex” (28.7%) groups were the most prevalent, followed by “*O*-heterocyclic” (26.3%), “hydroxanthenes” (9.9%), and “prenylated” (6.4%) (Figure 2a).

Simple xanthenes

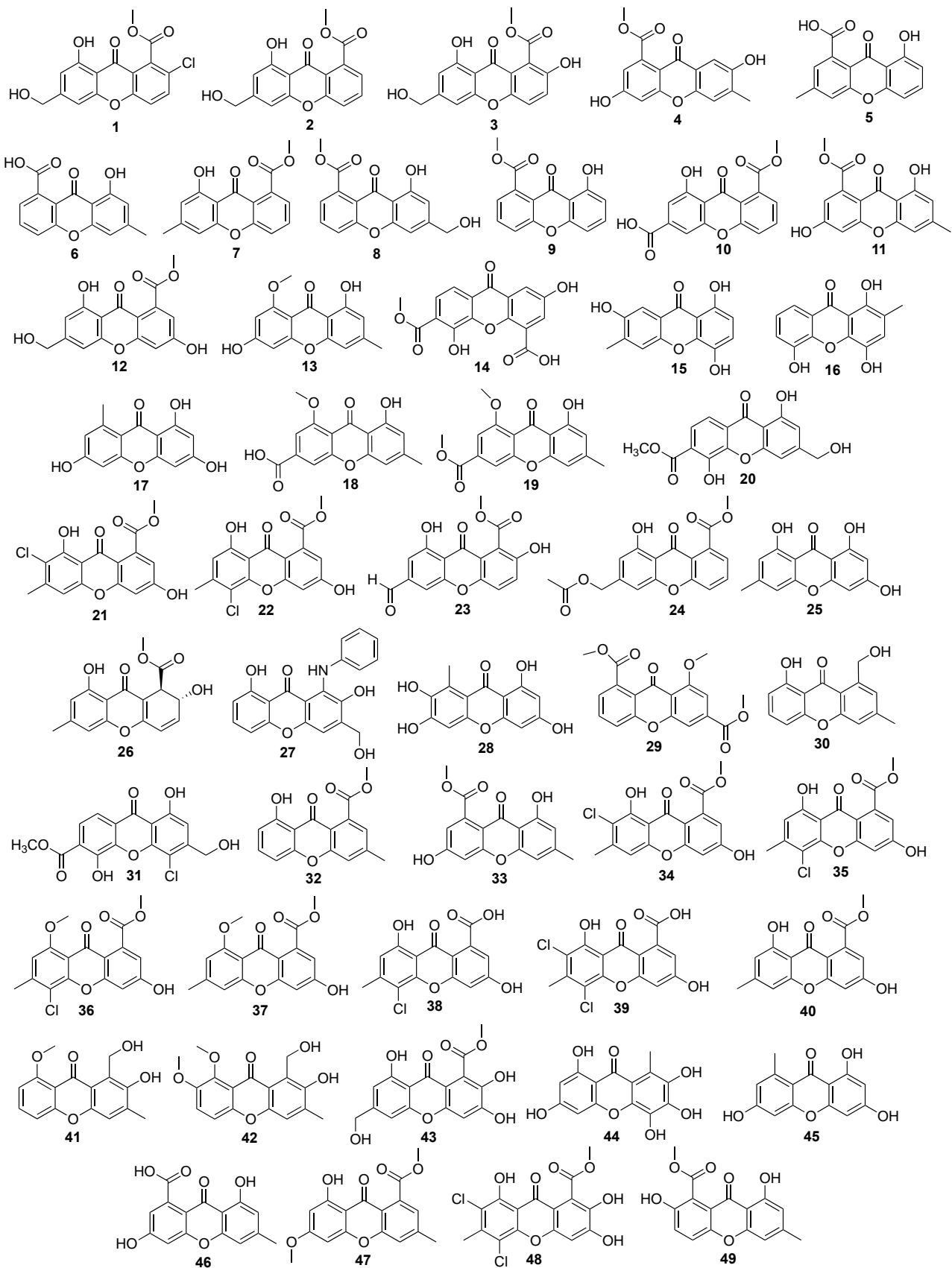
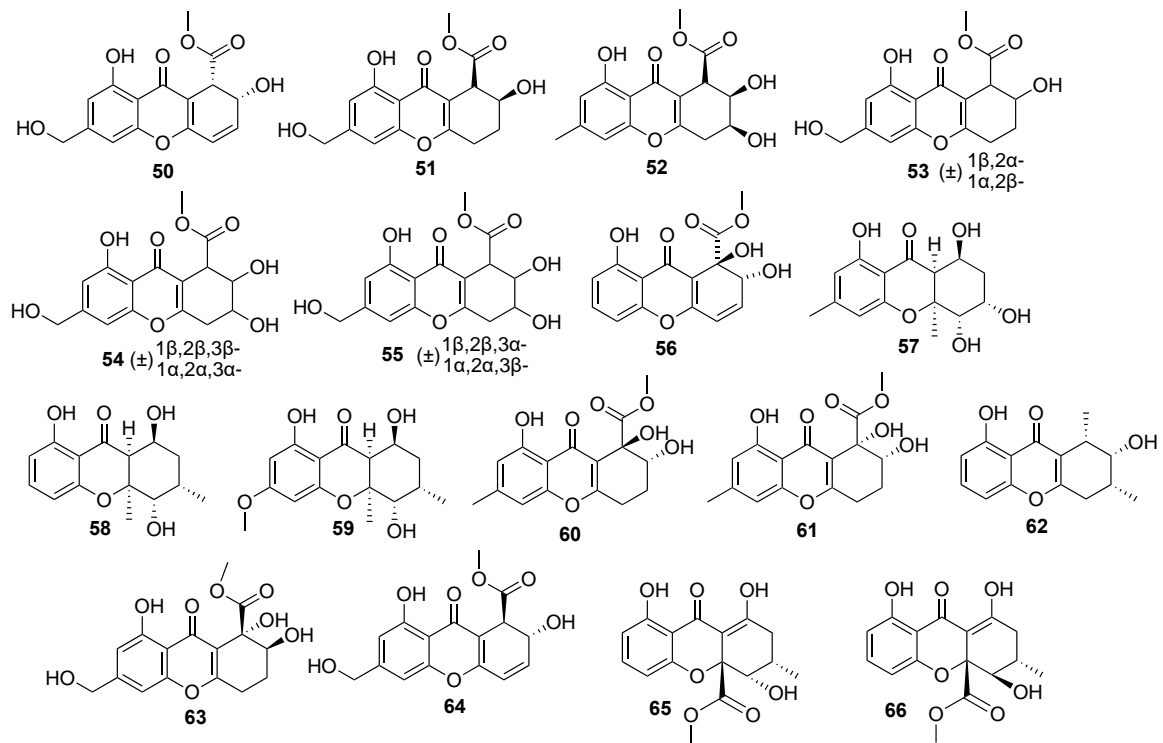
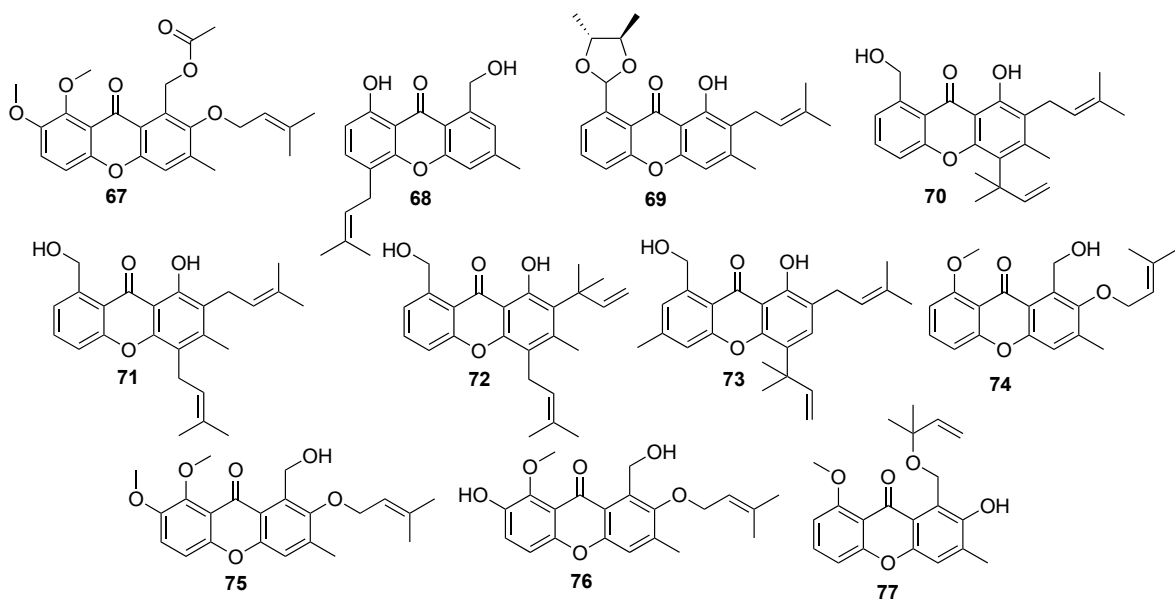


Figure 1. Cont.

Hydroxanthones



Prenylated xanthenes



O-Heterocyclic xanthenes

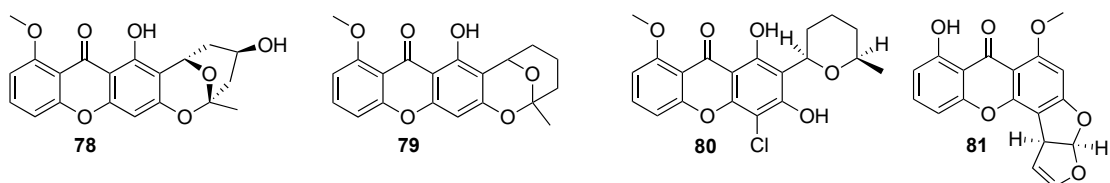


Figure 1. Cont.

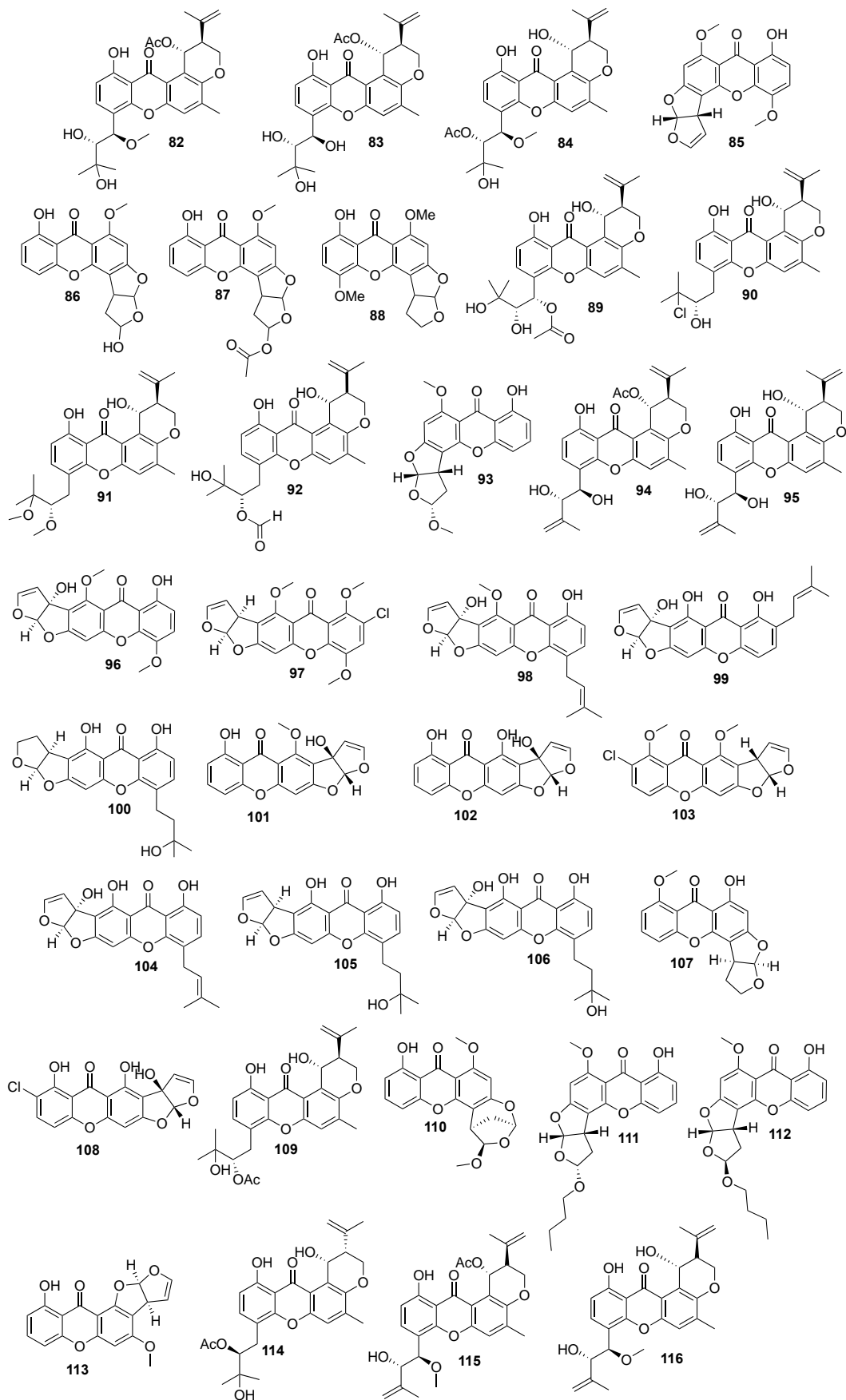
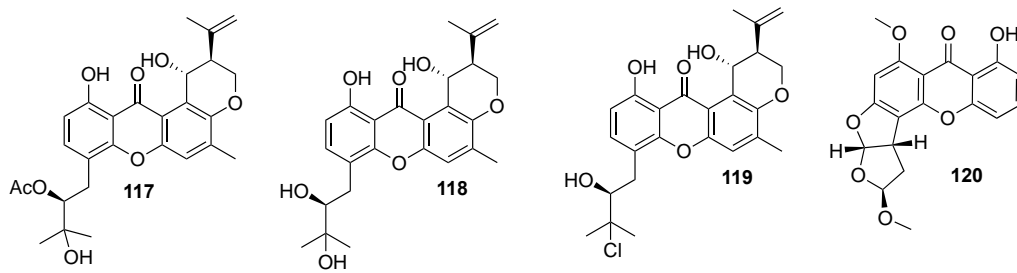


Figure 1. Cont.



Complex xanthones

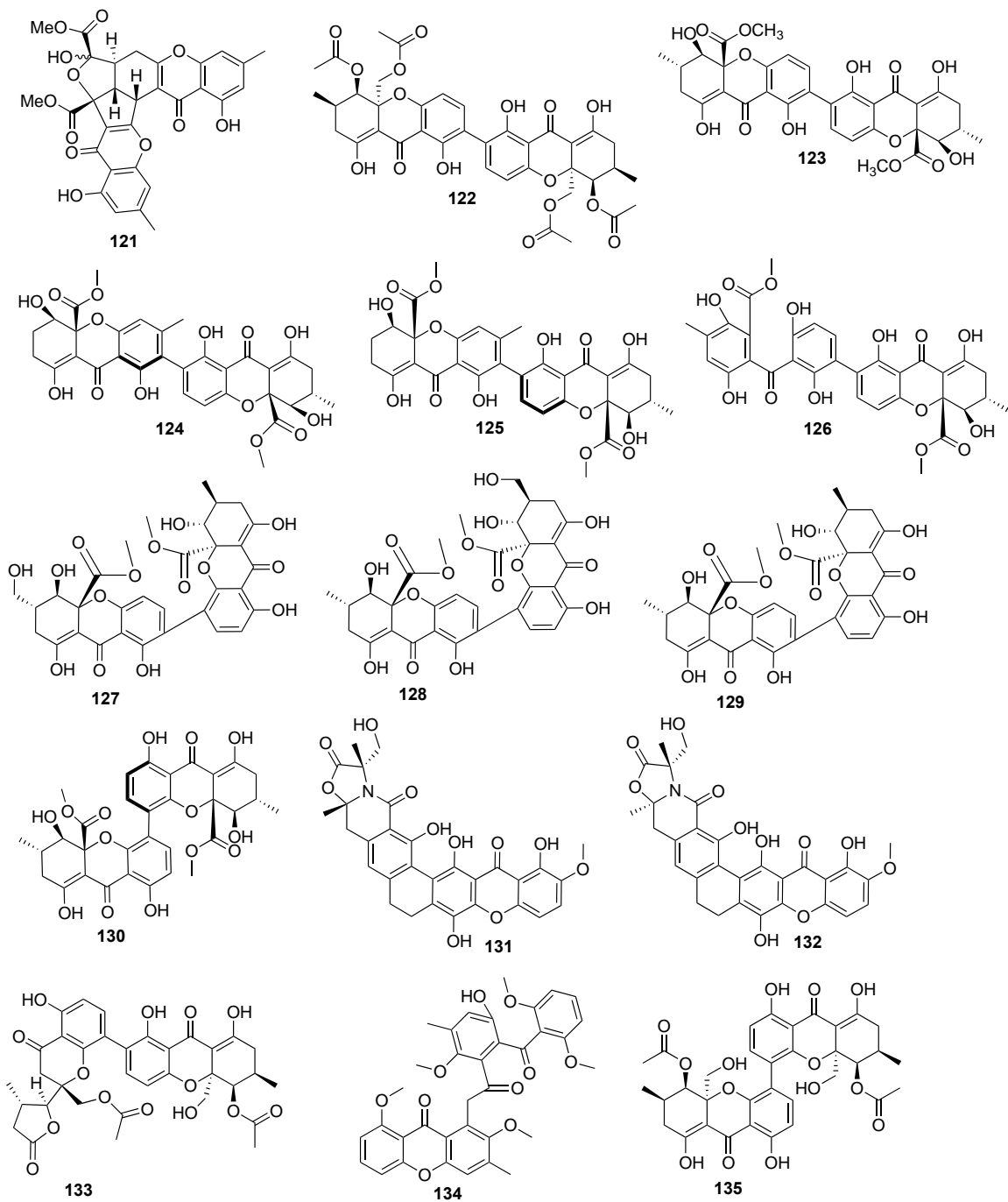


Figure 1. Cont.

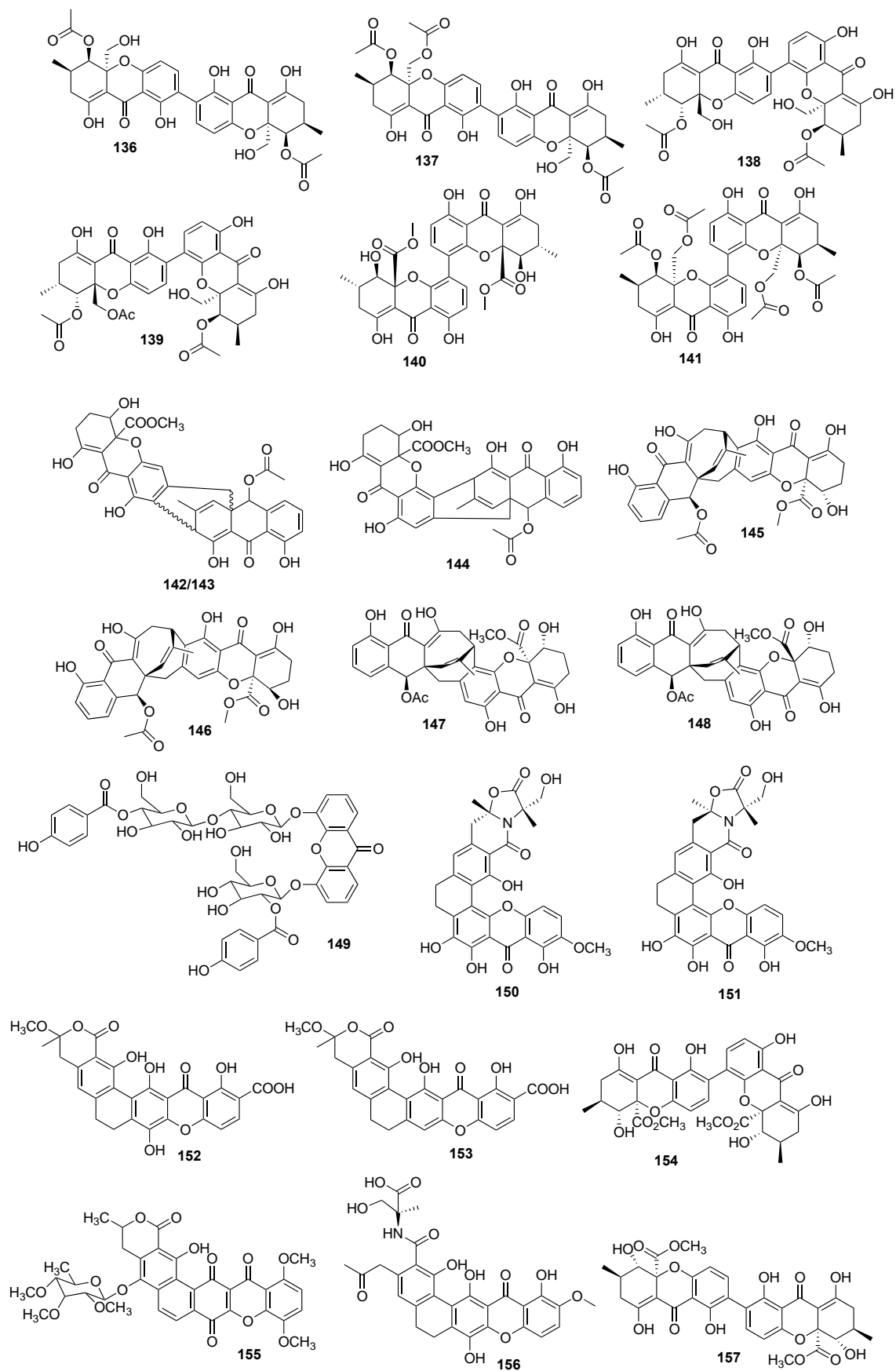


Figure 1. Cont.

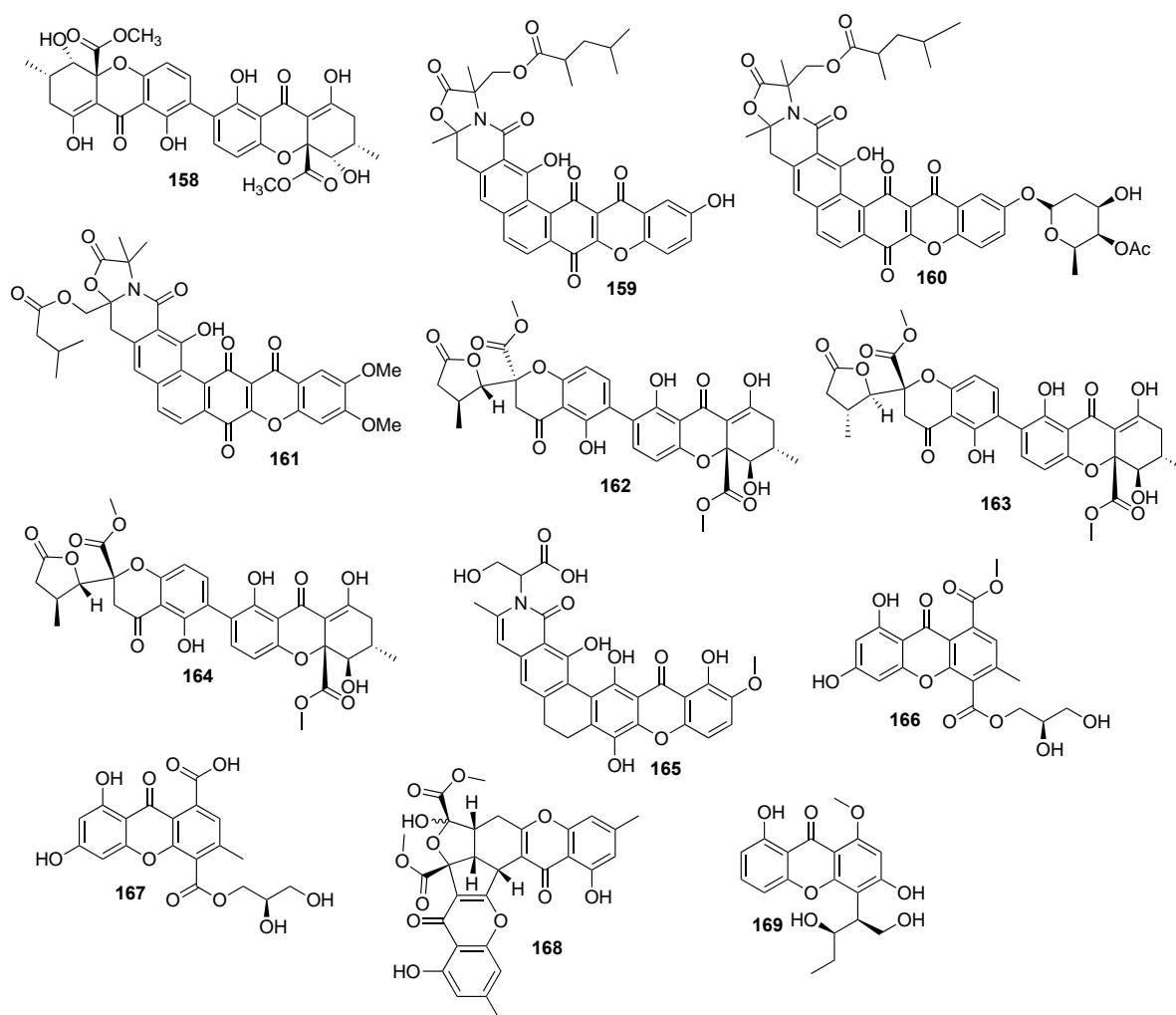


Figure 1. Structures of bioactive marine xanthenes.

The bioactive marine xanthenes were mostly isolated from marine fungi, namely from fungi belonging to the *Aspergillus* genus (41%, Figure 2b). Only a few examples were isolated from bacteria, and among them, the *Streptomyces* genus was the source that provided more bioactive xanthenes (4.5%). Half of the reported bioactive marine xanthenes (53%) were isolated from endophytic microorganisms associated with macroorganisms, like mangroves (39 marine xanthenes), sponges (38 marine xanthenes), algae (16 marine xanthenes), corals (12 marine xanthenes), jellyfish (1 marine xanthone), and seaweed (1 marine xanthone).

As specialized metabolites, xanthenes are often used as chemical defense agents. The most prevalent described activities were antitumor (43.5%) and antimicrobial (antibacterial (31.7%), antifungal (12.4%), and antiviral (10.6%) which provides some sort of protection to other competitive or predator marine organisms (Figure 2c). Interestingly, 22% of the identified marine xanthenes presented more than one biological activity (sum of all activities >100% in Figure 2c).

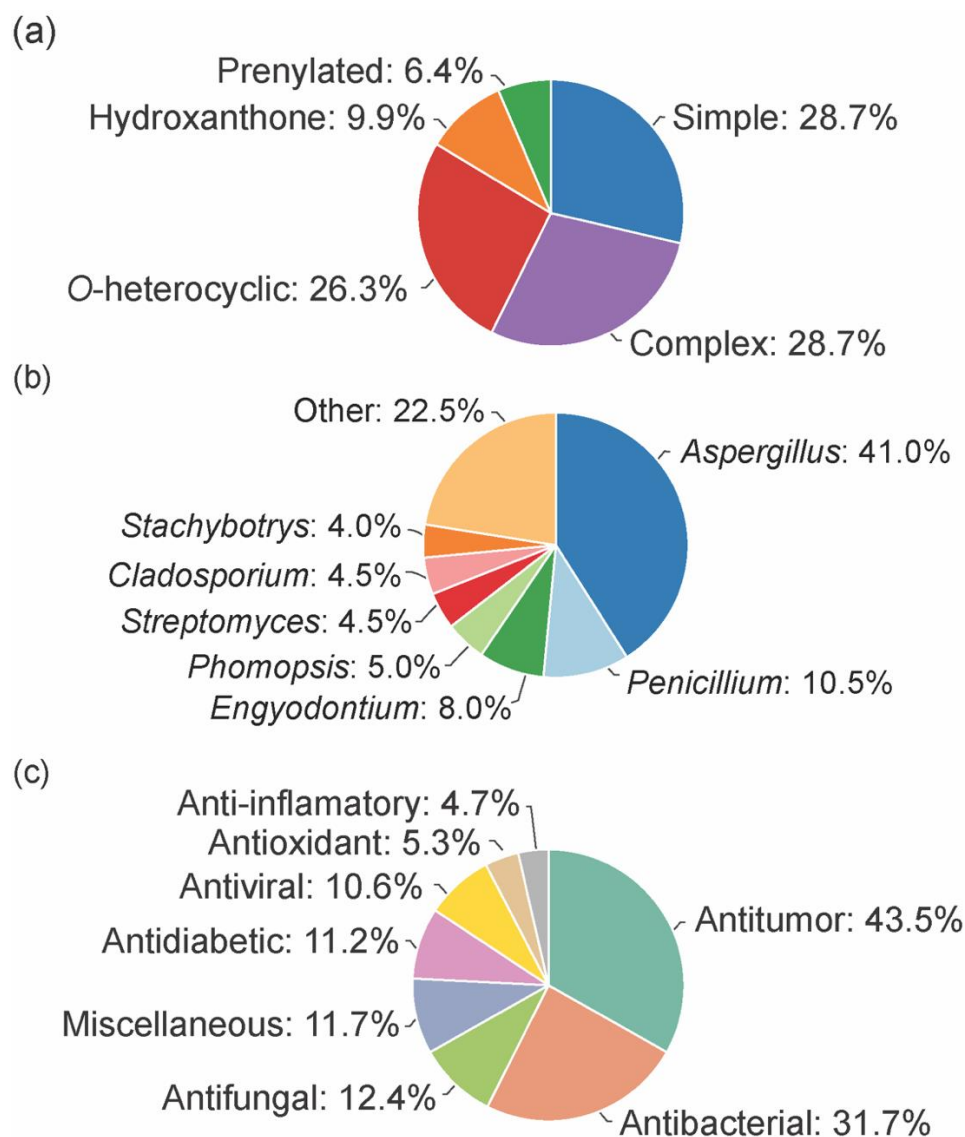


Figure 2. Distribution of type (a) microorganism source (b) and activity (c) of the bioactive marine xanthenes.

3. Chemical Space of Bioactive Marine Xanthenes

Bioactive marine xanthenes are produced by and act in living organisms, and to fulfill their specific biological task, they are structurally optimized by nature. Therefore, defining their chemical space is important for designing new molecules with desirable properties and pharmacological potential.

To describe the chemical space occupied by bioactive marine xanthenes, several molecular descriptors, embracing different molecular, physico-chemical, and topological properties, were calculated using the RDKit (release 2021_03_5 Q1 2021) and SwissADME [17]. For each marine xanthone, the following molecular descriptors were calculated: molecular weight (MW), fraction of sp³ carbons (Fsp³), number of rotatable bonds (RB), lipophilicity (Log P), topological polar surface area (TPSA), and solubility (Log S) (Table S1). The molecular descriptors were analyzed accordingly to the structural type of xanthenes (Figure 3).

Molecular size can be expressed in terms of MW, which is a predictor for pharmacokinetics behavior because bioavailability usually decreases as the molecular size increases [18]. In terms of size, the majority of the marine xanthenes presented MWs within the range of 300 to 600 g·mol⁻¹. “Complex” xanthenes presented the highest mean value (621.7 g·mol⁻¹) and the highest value dispersion (standard deviation of 85) due to the inclu-

sion of several dimeric and glycosylated structures. On the other side, “simple” xanthenes and “hydroxanthenes” have the lowest MW mean values (306.9 and 311.2 g·mol⁻¹, respectively) as these xanthenes are composed by the xanthenic nucleus with simple substituents (such as hydroxyl or methyl or methoxy group).

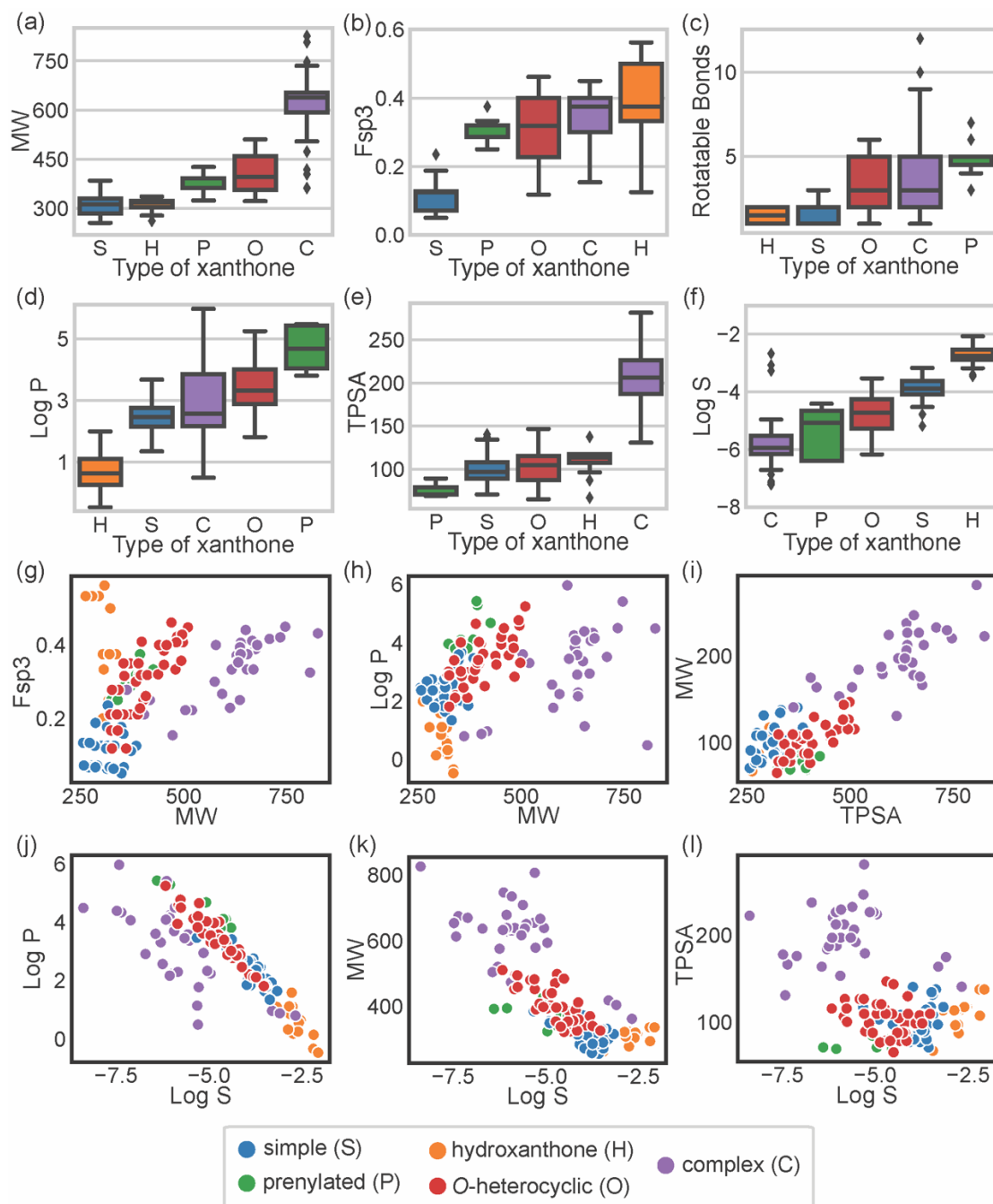


Figure 3. Distribution of MW (a); Fsp³ (b); number of RBs (c); log P (d); TPSA (e); and log S (f) accordingly to the type of xanthone: “simple” (S, blue), “prenylated” (P, green), “hydroxanthone” (H, orange), O-heterocyclic (O, red), and complex (C, purple). Comparison between the values of Fsp³ carbons and MW (g); log P and MW (h); MW and TPSA (i); log P and log S (j); MW and log S (k); TPSA and log S (l).

Molecular flexibility depends primarily on carbon saturation (Fsp³) and on the number of rotatable bonds (RB). A high number of RB and/or Fsp³ means that the molecule has conformation flexibility which results in a less planar, less rigid, and more com-

plex three-dimensional shape. Both RB and Fsp³ are important for determining oral bioavailability [10,19]. “Simple” xanthenes have the lowest Fsp³ values (mean value of 0.11) as saturated bonds are only present in substituent groups (Figure 3b). “Prenylated” and “O-heterocyclic” xanthenes have equal mean Fsp³ values (mean values of 0.31), but the latter showed higher value dispersion (interquartile range of 0.03 for “prenylated” and 0.17 for “O-heterocyclic” xanthenes, Figure 3b), which is a consequence of higher 3D complexity rather than larger size (Figure 3g). “Complex” xanthenes have a high value dispersion (standard deviation of 0.07, Figure 3b) due to their wide range of sizes (Figure 3g). Fsp³ values greater than 0.42 are considered to be suitable values for a drug [19], and half of the “hydroxanthenes” obey this criterion. In agreement with Fsp³ analysis, “O-heterocyclic”, “complex”, and “prenylated” xanthenes have a higher number of freely rotating bonds (median values of 3, 3, and 5 for “O-heterocyclic”, “complex”, and “prenylated”, respectively). “Hydroxanthenes” have the highest Fsp³ values (median value of 0.38), but they have the lowest number of RB (median value of 1.50), meaning that saturated bonds belong to the cyclic system of the hydroxanthonic nucleus (Figure 3c). Good oral absorption is associated with a number of RBs < 10 [10], and the vast majority of the marine xanthenes fulfill this criterion.

Lipophilicity, assessed by log P, is a key parameter that affects both pharmacodynamics and pharmacokinetics [20]. “Hydroxanthone” (mean value of 0.68) and “simple” xanthenes (mean value of 2.48) have the lowest log P values as they are frequently substituted with hydrophilic groups (hydroxyl and carboxylic). “O-heterocyclic” xanthenes presented log P values similar (median value of 3.32) to the xanthone itself (calculated log P of 2.95), meaning that the additional O-heterocyclic moiety does not contribute significantly to lipophilicity. “Prenylated” xanthenes have the highest log P value (mean value of 4.68), significantly higher than the “O-heterocyclic”. “Complex” xanthenes (median of 2.57) present the highest dispersion of log P values (standard deviation of 1.2), putting in evidence their structural diversity. The increase or decrease lipophilicity of marine xanthenes is dependent on the substitution pattern, namely on the presence of hydrophilic or lipophilic substitutions. The size of the marine xanthone was not correlated with increasing lipophilicity as different sized molecules have quite similar log P values (Figure 3h), such as compound 10 (314 g·mol⁻¹, log P 2.14) and compound 157 (638 g·mol⁻¹, log P 2.16).

Molecular polarity, evaluated as the sum of surfaces of polar atoms in a molecule (TPSA), has been used to predict the permeability of drugs [21]. Different xanthone types have quite similar mean TPSA values (ranged from 74.8 Å² for “prenylated” up to 110.7 Å² for “hydroxanthenes”), with the exception of complex xanthenes that have significantly higher values (mean value of 203.9 Å²) (Figure 3e). “Complex” xanthenes are the only type that violates the preconized 140 Å² limit value [10]. In marine xanthenes, the polarity is mostly related to MW, as TPSA values increase almost linearly with the MW (Figure 3i). In the case of marine xanthenes, this is attributed to the increased number of polar atoms, such as oxygen or nitrogen, with increasing MW.

The water solubility, expressed as log S, is an important parameter for drug bioavailability. Compounds with poor water solubility have poor absorption and oral bioavailability, the evaluation of their bioactivity might be erratic, and the formulation development will be challenging [22]. The solubility trend observed with marine xanthenes was: “hydroxanthenes” > “simple” > “O-heterocyclic” > “prenylated” > “complex”. “Hydroxanthenes” were the most soluble group (mean value of -2.74), while “complex” xanthenes were the most poorly soluble group (mean value of -5.84) (Figure 3f). “Simple” and “hydroxanthenes” are above the log S value of -4, which is considered an acceptable value for a drug [23]. This trend is related to lipophilicity (Figure 3j) and size (Figure 3k). The poor solubility of complex xanthenes is ascribed to their high molecular weight and high lipophilicity, while the smaller and/or more hydrophilic hydroxanthenes have good water solubility (Figure 3f). Solubility of marine xanthenes seems not to be affected by polarity as log S and TPSA were not correlated (Figure 3l).

NP-likeness allows measuring the similarity of a molecule to natural products [15]. The NP-likeness score quantifies this similarity; the higher the score, the higher the resemblance of that molecule to an NP [15]. NP-likeness scores of marine xanthenes were calculated using the web service NaPles [24]. Figure 4a depicts the probability density function, based on kernel density estimation (KDE), of NP-likeness score for all NPs and synthetic molecules (SMs), as well as the score of marine xanthenes. As expected, the NP-likeness score of marine xanthenes falls within the range of NP. NP-likeness score of marine xanthenes was analyzed considering the different types of xanthenes (Figure 4b). Xanthone itself is similar to SMs (NP-likeness score of 0.19), while hexahydroxanthone presents a high score (NP-likeness score of 1.57). Within marine xanthenes, “simple” xanthenes have the lowest similarity with NP molecules (mean score of 1.09). The extension of the degree of substitution, from the simple hydroxyl groups in “simple” xanthenes, up to an additional xanthonic nucleus present in “complex” xanthenes, leads to the increase in the similarity to NP. This is in agreement with the fact that usually, NP are structurally more complex than synthetic molecules [25].

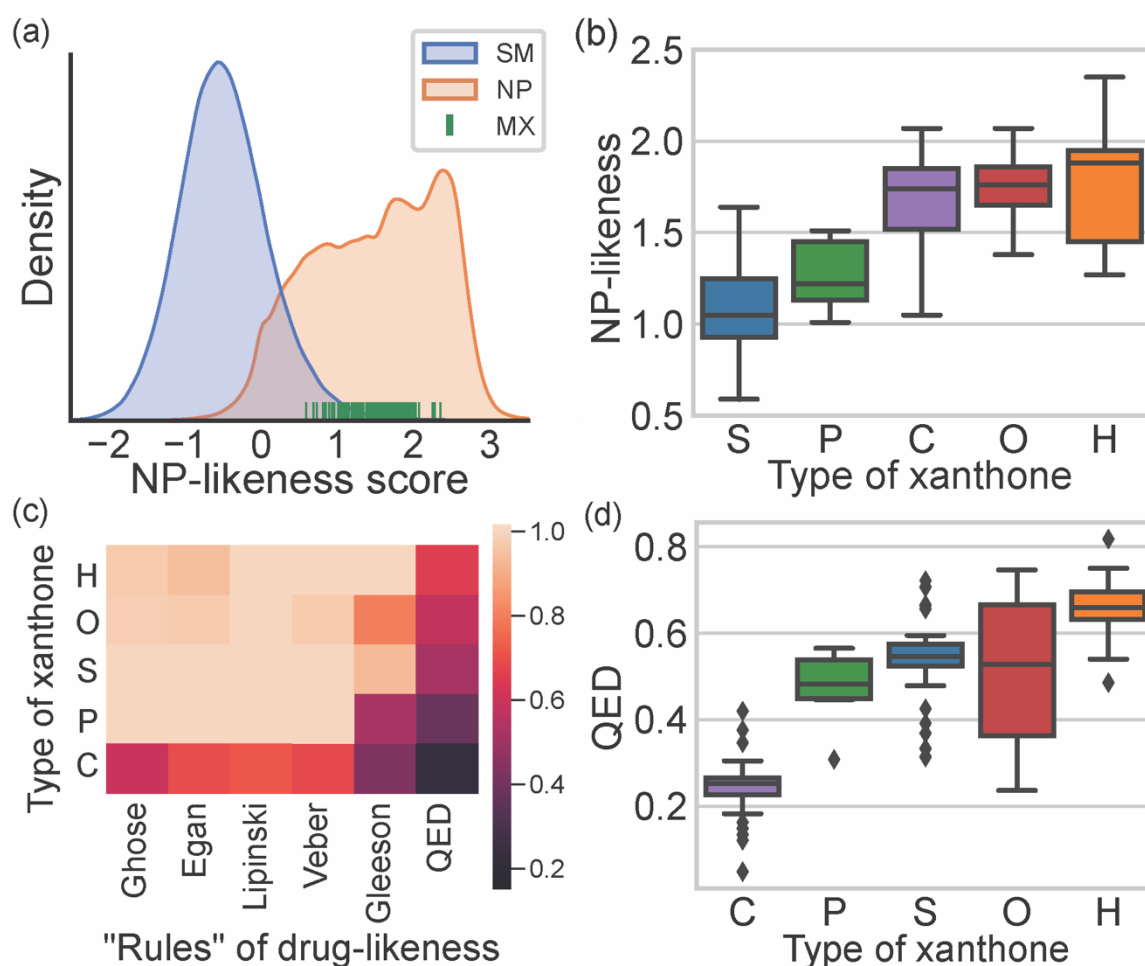


Figure 4. (a) KDE distribution plot NP-likeness score of synthetic molecules (SM), natural products (NP), and NP-likeness score of marine xanthenes. (b) Distribution of NP-likeness score accordingly to the type of xanthone: “simple” (S, blue), “prenylated” (P, green), “hydroxanthone” (H, orange), “O-heterocyclic” (O, red), and “complex” (C, purple). (c) Heatmap of the compliance with rules of drug-likeness for the xanthone types. (d) Distribution of QED index accordingly to the type of xanthone.

Drug-likeness allows estimating the probability of a molecule to become a drug administered orally [17]. The classical approach to drug-likeness is normally based on a set of criteria to which the compounds under study should obey. This approach provides a

binary “yes or no” assessment, depending on if the compound obeys or not the preconized limit values. Drug-likeness of marine xanthenes were evaluated considering the classical Lipinski [9], Veber [10], Ghose [11], Egan [12], and Gleeson rules [13]. In this study, a compliance value, defined as 0 when a compound does not obey any of the preconized criteria of that rule and 1 when a compound fulfills all criteria, was calculated for each marine xanthenes (Table S2). Figure 4c displays the obtained mean compliance values of each type of marine xanthenes for each rule. A lighter color in the heatmap plotted in Figure 4c means higher compliance, while a darker color means less compliance. “Hydroxanthone”, “O-heterocyclic”, “simple”, and “prenylated” xanthenes meet most of the criteria defined by classical rules, except for the Gleeson rules. On the contrary, “complex” xanthenes violate at least one criterion in all the considered rules (Figure 4c). Among the classical rules, the Gleeson rules [13] were the best to discriminate the different types of xanthenes. “Simple” and “hydroxanthones” obey most of the criteria, “prenylated” obey just some, and “complex” xanthenes do not obey the generality of Gleeson’s proposed criteria.

Classical rules have many exceptions, and there are many examples, namely among NP or NP-inspired, of successful drugs that violate them [26]. Quantitative estimate of drug-likeness (QED) is an alternative way for assessing drug-likeness. QED index is generated considering eight properties, namely MW, log P, TPSA, RB, number of hydrogen donors and acceptors, number of aromatic rings, and number of alerts for undesirable substructures [14]. Compared with classical drug-likeness rules, the QED method is more flexible because it does not use cutoffs but a continuous score index of drug-likeness. When all properties are unfavorable, the QED index is 0, and when all properties are favorable, the score is 1 [14]. The obtained QED indexes for marine xanthenes clearly differentiate the distinct types (Table S2, Figure 4c,d), enabling sorting the marine xanthenes in the following ascending order of drug-likeness: “complex”, “prenylated”, “simple”, “O-heterocyclic”, and “hydroxanthones”. The low drug-likeness of “complex” marine xanthenes is related to their high MW (Figure 3a) and low solubility (Figure 3f), while the drug-likeness of “hydroxanthones” is ascribed to their low lipophilicity (Figure 3d) and good water solubility (Figure 3f).

Considering the reported biological activities of marine xanthenes, the relationship between these and the molecular descriptors was established. Figure 5a–d displays the relationship of the most relevant molecular descriptors (MW, log S, log P, and F_{sp^3}) with the most representative biological activities (antitumor, antibacterial, antifungal, antiviral, and antidiabetic). As the number of xanthenes reported for each biological activity is different, the results should only be compared when the number of reported molecules is similar (antitumor vs. antibacterial and antifungal vs. antiviral vs. antidiabetic).

Antitumor marine xanthenes have a bimodal distribution of MW with 2 subsets of different sized compounds (one mode of 314.3 g mol^{-1} and another mode of 636.6 g mol^{-1}) (Figure 5a). The presence of a bimodal distribution is also observed for the solubility of antitumor marine xanthenes (modes of -3.45 and -5.66) (Figure 5b), which is not surprising considering that log S and MW are strictly correlated (Figure 3k). However, log P have a unimodal distribution with a mode of 2.33 (Figure 5c). Similarly, antibacterial marine xanthenes also showed a bimodal distribution of MW (modes of 336.3 and 628.6 g mol^{-1}) and log S values (modes of -4.23 and -5.84) (Figure 5a,b) and a unimodal distribution of log P values (mode of 2.37) (Figure 5c). The features of the large-sized subset of antitumor/antibacterial marine xanthone, i.e., “obese” molecules that apparently violate drug-likeness but with a suitable log P value, is a trait of NPs molecules. Despite being often cited as exceptions to classical drug-likeness rules, NP molecules largely comply in terms of log P [27]. This is attributed to the way in which natural evolution took place, producing bioactive compounds that retain low hydrophobicity, even for molecules with high MW [27]. The major difference between the physicochemical properties of antitumor and antibacterial xanthenes was in terms of carbon saturation. Antibacterial marine xanthenes have lower and more dispersed F_{sp^3} values than antitumor xanthenes (median value of 0.38 and 0.32

for antibacterial and antitumor, respectively), raising the hypothesis that more rigidity might be an important aspect for the antibacterial activity (Figure 5d).

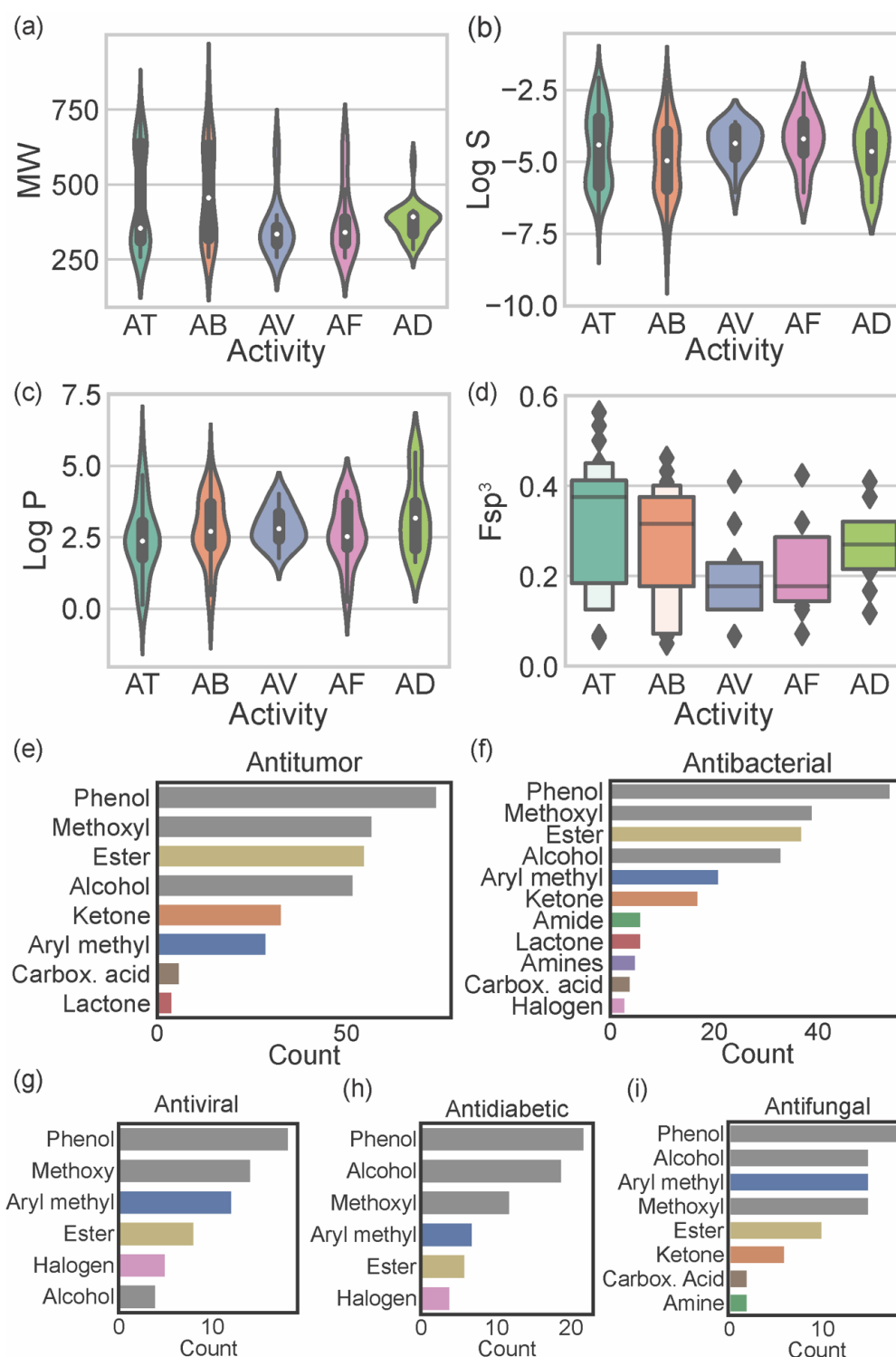


Figure 5. Distribution of MW (a); log S (b); log P (c); and fraction of sp³ carbons (d) accordingly to the biological activity reported for marine xanthenes: antitumor (AT), antibacterial (AB), antiviral (AV), antifungal (AF), and antidiabetic (AD). Analysis of the functional group frequently found on antitumor (e); antibacterial (f); antiviral (g); antifungal (h), and antidiabetic (i) marine xanthenes.

Antiviral, antifungal, and antidiabetic marine xanthenes presented a unimodal distribution of MW values representing only one set of similar-sized compounds (mode values

ranged from 334.7 to 394.5 g mol⁻¹) (Figure 5a). Antidiabetic xanthenes have a narrower probability distribution of the MW values (Figure 5a), and antiviral xanthenes have a narrower dispersion of log S probability distribution (Figure 5b) and of log P probability distribution (Figure 5c). Antiviral and antifungal marine xanthenes tend to be quite rigid molecules as they show the lowest Fsp³ values (median values of 0.18, Figure 5d). Antiviral, antifungal, and antidiabetic marine fulfill the limited preconized by the drug-likeness filters independently of the descriptor.

The most representative heteroatom in marine xanthenes is the oxygen atom, distributed by phenols (present in 96.5% of the reported marine xanthenes), methoxy groups (67.8%), alcohols (63.7%), esters (58.5%), ketones (26.9%), and carboxylic acids (7.0%) (Table S3). Other heteroatoms, different from oxygen, present in marine xanthenes are halogens (9.4%), mainly the chloride atom, followed by the nitrogen atom, distributed by amines (10 marine xanthenes) and amides (8 marine xanthenes). The distribution of chemical functional groups by biological activities of marine xanthenes was analyzed (Figure 5e–i). The most prevalent functional groups in antitumor, antibacterial, and antiviral xanthenes are phenolic and methoxy groups (grey bars on Figure 5e–g). The most prevalent functional groups in antidiabetic and antifungal are phenolic and alcohol groups (grey bars on Figure 5h,i). Esters are very common in xanthenes independent of biological activity. Ketones and aryl methyl groups are common in antitumor, antibacterial, and antifungal marine xanthenes (Figure 5e,f,i). Halogens are present in some antiviral and antidiabetic xanthenes. Nitrogen-containing groups, like amide and amines, are present in antibacterial and antifungal xanthenes. Amine groups, which are protonated at physiological pH, could be important for the anti-infective activity of the marine xanthenes bearing this group.

4. Biological Activities of Marine Xanthenes

A total of 74 marine xanthenes described in literature were evaluated for antitumor activity, measuring their growth inhibitory activity in different tumor cell lines (Table 1). The cervical carcinoma cell line (HeLA), human lung carcinoma (A549), human breast adenocarcinoma cell line (MCF-7), and human leukemia cell line (HL-60) were the most used tumor cell lines in the biological assays (Figure 6). The number of xanthenes with a half maximum inhibitory concentration (IC₅₀) lower than 10 μM varied depending on the tested cell lines. For instance, the number of xanthenes screened against HL-60, MCF-7, and Huh7 cells was almost the same, but the number of most potent xanthenes was higher identified against HL-60 cells. None of the marine xanthenes assayed against C4-2B, 22RV1, and RWPE-1 presented an IC₅₀ lower than 10 μM, while for MGC-803, the most part presented an IC₅₀ lower than 10 μM.

Table 1. Antitumor marine xanthenes.

Name	Activity	Source	Ref.
Engyodontiumone B (1)	U937 (IC ₅₀ = 55.5 μM); HeLa (IC ₅₀ = 96.1 μM); MCF-7 (IC ₅₀ = 172.3 μM); HepG2 (IC ₅₀ = 73.8 μM); Huh7 (IC ₅₀ ≥ 300 μM)		
Sydowinin A (2)	U937 (IC ₅₀ = 75.6 μM); HeLa (IC ₅₀ ≥ 300 μM); MCF-7 (IC ₅₀ ≥ 300 μM); HepG2 (IC ₅₀ ≥ 300 μM); Huh7 (IC ₅₀ ≥ 300 μM)	<i>Engyodontium album</i> (DFFSCS02) isolated from sediment collected in the South China Sea	[28]
Sydowinin B (3)	U937 (IC ₅₀ = 127.0 μM); HeLa (IC ₅₀ ≥ 300 μM); MCF-7 (IC ₅₀ ≥ 300 μM); HepG2 (IC ₅₀ ≥ 300 μM); Huh7 (IC ₅₀ ≥ 300 μM)		
2,6-Dihydroxy-3-methyl-9-oxoxanthene-8-carboxylic acid methyl ester (4)	HEp-2 (IC ₅₀ = 8 μg mL ⁻¹); HepG2 (IC ₅₀ = 9 μg mL ⁻¹)	Endophytic fungus (SK7RN3G1) isolated from mangrove collected in the South China Sea	[29]

Table 1. Cont.

Name	Activity	Source	Ref.
Monodictyxanthone (5)	Hepa-1c1c7(Cyp1A inhibition ($IC_{50} = 34.8 \pm 7.4 \mu M$); NAD(P)H:quinone reductase induction ($CD \geq 50 (1.4) \mu M$, $IC_{50} \geq 50 \mu M$)	<i>Monodictys putredinis</i> isolated from the inner tissue of a green alga collected at Tenerife	[30]
8-Hydroxy-6-methylxanthone-1-carboxylic acid (6)	% Inhibitions on the cell proliferation at 10 μM : 22RV1 ($71.3 \pm 1.2\%$); C4-2B ($60.7 \pm 5.1\%$); RWPE-1 ($19.7 \pm 4.9\%$)		
Methyl 8-hydroxy-6-methyl-9-oxo-9H-xanthene-1-carboxylate (7)	% Inhibitions on the cell proliferation at 10 μM : 22RV1 ($55.8 \pm 3.0\%$); C4-2B ($8.1 \pm 20.6\%$); RWPE-1 ($5.3 \pm 3.1\%$)		
Methyl 8-hydroxy-6-(hydroxymethyl)-9-oxo-9H-xanthene-1-carboxylate (8)	% Inhibitions on the cell proliferation at 10 μM : 22RV1 ($68.1 \pm 1.9\%$); C4-2B ($20.2 \pm 0.1\%$); RWPE-1 ($19.0 \pm 8.5\%$)		
Vertixanthone (9)	% Inhibitions on the cell proliferation at 10 μM : 22RV1 ($27.1 \pm 6.9\%$); C4-2B ($-0.1 \pm 4.6\%$); RWPE-1 ($25.0 \pm 7.9\%$)	<i>Cladosporium halotolerans</i> (GXIMD 02502) isolated from a coral collected in Beibu Gulf	[31]
8-(Methoxycarbonyl)-1-hydroxy-9-oxo-9H-xanthene-3-carboxylic acid (10)	% Inhibitions on the cell proliferation at 10 μM : 22RV1 ($63.9 \pm 2.2\%$); C4-2B ($12.2 \pm 5.2\%$); RWPE-1 ($27.0 \pm 5.1\%$)		
3,8-Dihydroxy-6-methyl-9-oxo-9H-xanthene-1-carboxylate (11)	% Inhibitions on the cell proliferation at 10 μM : 22RV1 ($82.1 \pm 0.9\%$); C4-2B ($77.7 \pm 0.5\%$); RWPE-1 ($11.5 \pm 1.5\%$)		
Conioxanthone A (12)	% Inhibitions on the cell proliferation at 10 μM : 22RV1 ($36.8 \pm 13.3\%$); C4-2B ($3.3 \pm 11.3\%$); RWPE-1 ($20.3 \pm 9.0\%$)		
Questin (13)	A549 ($IC_{50} = 40.0 \pm 0.3 \mu M$); HepG2 ($IC_{50} = 42.2 \pm 0.5 \mu M$); HeLa ($IC_{50} = 36.2 \pm 0.9 \mu M$)	<i>Aspergillus sydowii</i> (C1-S01-A7) collected in the West Pacific Ocean	[32]
Penixanacid A (14)	HeLa ($IC_{50} = 10.0 \mu M$); BEL-7402 ($IC_{50} = 30.6 \mu M$); HEK-293 ($IC_{50} = 28.5 \mu M$); HCT-116 ($IC_{50} = 19.0 \mu M$); A-549 ($IC_{50} = 16.9 \mu M$)	<i>Penicillium chrysogenum</i> (HND11-24) isolated from a mangrove	[33]
Norlichexanthone (17)	K562 ($IC_{50} = 74.6 \mu M$); A549 ($IC_{50} = 64.6 \mu M$); Huh-7 ($IC_{50} > 30 \mu M$); H1975 ($IC_{50} = 79.1 \mu M$); MCF-7 ($IC_{50} = 56.7 \mu M$); U937 ($IC_{50} > 30 \mu M$); BGC823 ($IC_{50} = 697.6 \mu M$); HL-60 ($IC_{50} > 30 \mu M$); MOLT-4 ($IC_{50} = 135.4 \mu M$); HeLa ($IC_{50} = 7.2 \mu M$)	<i>Stachybotry</i> sp. (ZSDS1F1-2) isolated from a sponge collected at Xisha Island	[34]
Yicathin C (18)	A549 ($IC_{50} = 37.7 \pm 0.3 \mu M$)	<i>Aspergillus sydowii</i> (C1-S01-A7) collected in the West Pacific Ocean	[32]
Yicathin B (19)	A375-C5 ($IC_{50} = 48.70 \pm 4.24 \mu M$); MCF-7 ($IC_{50} = 98.93 \pm 9.83 \mu M$); NCI-H460 ($IC_{50} = 79.83 \pm 18.45 \mu M$)	<i>Aspergillus wentii</i> isolated from <i>Gymnogongrus flabelliformis</i> collected at Pingtan Island	[4]
2-Hydroxy-6-formyl-vertixanthone (23)	HepG2 ($IC_{50} = 32.7 \pm 0.9 \mu M$)		
12-O-Acetyl-sydowinin A (24)	A549 ($IC_{50} = 25.2 \pm 0.9 \mu M$); HepG2 ($IC_{50} = 42.3 \pm 0.6 \mu M$); HeLa ($IC_{50} = 33.6 \pm 0.7 \mu M$)	<i>Aspergillus sydowii</i> (C1-S01-A7) collected in the West Pacific Ocean	[32]
Emodin (25)	HeLa ($IC_{50} = 27.1 \pm 0.8 \mu M$)		
Engyodontiumone H (50)	U937 ($IC_{50} = 4.9 \mu M$); HeLa ($IC_{50} = 24.8 \mu M$); MCF-7 ($IC_{50} = 38.5 \mu M$); HepG2 ($IC_{50} = 60.5 \mu M$); Huh7 ($IC_{50} = 53.3 \mu M$)		
Engyodontiumone C (51)	U937 ($IC_{50} = 218.4 \mu M$); HeLa ($IC_{50} \geq 300 \mu M$); MCF-7 ($IC_{50} \geq 300 \mu M$); HepG2 ($IC_{50} \geq 300 \mu M$); Huh7 ($IC_{50} \geq 300 \mu M$)	<i>Engyodontium album</i> (DFSCS021) from isolated sediment collected in the South China Sea	[28]
Engyodontiumone D (52)	U937 ($IC_{50} = 208.6 \mu M$); HeLa ($IC_{50} \geq 300 \mu M$); MCF-7 ($IC_{50} \geq 300 \mu M$); HepG2 ($IC_{50} \geq 300 \mu M$); Huh7 ($IC_{50} \geq 300 \mu M$)		

Table 1. Cont.

Name	Activity	Source	Ref.
Engyodontiumone E (53)	U937 (IC ₅₀ = 15.9 µM); HeLa (IC ₅₀ = 205.9 µM); MCF-7 (IC ₅₀ ≥ 300 µM); HepG2 (IC ₅₀ ≥ 300 µM); Huh7 (IC ₅₀ ≥ 300 µM)		
Engyodontiumone F (54)	U937 (IC ₅₀ = 192.7 µM); HeLa (IC ₅₀ ≥ 300 µM); MCF-7 (IC ₅₀ ≥ 300 µM); HepG2 (IC ₅₀ ≥ 300 µM); Huh7 (IC ₅₀ ≥ 300 µM)	<i>Engyodontium album</i> (DFFSCS021) from isolated sediment collected in the South China Sea	[28]
Engyodontiumone G (55)	U937 (IC ₅₀ = 287.2 µM); HeLa (IC ₅₀ ≥ 300 µM); MCF-7 (IC ₅₀ ≥ 300 µM); HepG2 (IC ₅₀ ≥ 300 µM); Huh7 (IC ₅₀ ≥ 300 µM)		
Globosuxanthone A (56)	HCT-15 (IC ₅₀ = 10.7 µM); T-cell leukemia Jurkat cells (IC ₅₀ = 2.3 µM)	<i>Beauveria bassiana</i> (TPU942) isolated from a piece of an unidentified sponge collected at Iriomote Island	[35]
Monodictysin A (57)	Hepa-1c1c7(Cyp1A inhibition IC ₅₀ ≥ 50 µM); NAD(P)H:quinone reductase induction (CD = 191.1 µM, IC ₅₀ ≥ 400 µM)		
Monodictysin B (58)	Hepa-1c1c7(Cyp1A inhibition IC ₅₀ = 23.3 ± 3.9 µM); NAD(P)H:quinone reductase induction (CD = 12.0 ± 4.8 µM, IC ₅₀ ≥ 50 µM)	<i>Monodictys putredinis</i> isolated from the inner tissue of a green alga collected at Tenerife	[30]
Monodictysin C (59)	Hepa-1c1c7(Cyp1A inhibition IC ₅₀ = 3.0 ± 0.7 µM); NAD(P)H:quinone reductase induction (CD = 12.8 ± 2.6 µM, IC ₅₀ ≥ 50 µM)		
α-Diversonolic ester (60)	% Inhibitions on the cell proliferation at 10 µM: 22RV1 (28.8 ± 10.3%); C4-2B (12.9 ± 12.6%); RWPE-1 (24.3 ± 3.3%)	<i>Cladosporium halotolerans</i> (GXIMD 02502) isolated from a coral collected in Beibu Gulf	[31]
β-Diversonolic ester (61)	% Inhibitions on the cell proliferation at 10 µM: 22RV1 (40.2 ± 1.5%); C4-2B (2.8 ± 2.2%); RWPE-1 (10.3 ± 3.8%)		
Penixanthone A (62)	Weak cytotoxicity against H1975, MCF-7, K562, HL7702 at concentration of 30 µM.	<i>Penicillium</i> sp. (SYFz-1) isolated from a mangrove sample	[36]
	K562 (IC ₅₀ = 6.97 µM); MCF-7 (IC ₅₀ = 11.7 µM); HeLa (IC ₅₀ = 1.39 µM); DU145 (IC ₅₀ = 2.69 µM); U937 (IC ₅₀ = 0.463 µM); H1975 (IC ₅₀ = 8.53 µM); SGC-7901 (IC ₅₀ = 9.43 µM); A549 (IC ₅₀ = 7.01 µM); MOLT-4 (IC ₅₀ = 5.26 µM); HL-60 (IC ₅₀ = 6.20 µM)	<i>Aspergillus</i> sp. (SCSIO Ind09F01)	[37]
AGI-B4 (64)	U937 (IC ₅₀ = 8.8 µM); HeLa (IC ₅₀ = 60.0 µM); MCF-7 (IC ₅₀ = 102.2 µM); HepG2 (IC ₅₀ = 52.7 µM); Huh7 (IC ₅₀ = 133.3 µM)	<i>Engyodontium album</i> (DFFSCS021) isolated from sediment collected in the South China Sea	[28]
	L5178Y (IC ₅₀ = 1.5 µM)	<i>Scopulariopsis</i> sp. isolated from solid rice cultures obtained from the Red Sea hard coral <i>Stylophora</i> sp.	[38]
Versicone G (67)	NB ₄ (IC ₅₀ = 15.6 µM); HL-60 (IC ₅₀ = 21.7 µM); HeLa (IC ₅₀ = 16.9 µM)	<i>Aspergillus versicolor</i> (HDN11-84) isolated from mangrove	[39]
Paeciloxanthone (68)	HepG2 (IC ₅₀ = 1.08 µg mL ⁻¹)	<i>Paecilomyces</i> sp. isolated from mangrove collected in the Taiwan Strait	[40]
Chaetoxanthone A (78)	L6-cells (IC ₅₀ = 59.1 µg/mL)		
Chaetoxanthone B (79)	L6-cells (IC ₅₀ > 90 µg/mL)	<i>Chaetomium</i> sp. isolated from the Greek alga collected at Santorini Island.	[41]
Chaetoxanthone C (80)	L6-cells (IC ₅₀ = 46.7 µg/mL)		

Table 1. Cont.

Name	Activity	Source	Ref.
Sterigmatocystin (81)	Bel-7402 (IC ₅₀ = 96.53 µg mL ⁻¹); NCIH-460 (IC ₅₀ = 72.52 µg mL ⁻¹)	Fungal strain (isolate 1850) isolated from a leaf of <i>Kandelia candel</i> collected in Hong Kong	[42]
	A-549 (IC ₅₀ = 1.86 µg mL ⁻¹); SK-OV-3 (IC ₅₀ = 2.53 µg mL ⁻¹); SK-MEL-2 (IC ₅₀ = 1.22 µg mL ⁻¹); XF-498 (IC ₅₀ = 2.75 µg mL ⁻¹); HCT-15 (IC ₅₀ = 4.61 µg mL ⁻¹)	<i>Aspergillus versicolor</i> isolated from <i>Petrosia</i> sp.	[43]
	A-549 (IC ₅₀ = 11.25 µg mL ⁻¹); SK-OV-3 (IC ₅₀ = 17.36 µg mL ⁻¹); SK-MEL-2 (IC ₅₀ = 14.33 µg mL ⁻¹); XF-498 (IC ₅₀ = 15.12 µg mL ⁻¹); HCT-15 (IC ₅₀ ≥ 30 µg mL ⁻¹)	<i>Aspergillus versicolor</i>	[44]
Aspergixanthone A (82)	A-549 (IC ₅₀ = 1.8 µM)		
Aspergixanthone C (83)	MDA-MB-231 (IC ₅₀ = 3.3 µM); MCF-7 (IC ₅₀ = 2.8 µM); MGC-803 (IC ₅₀ = 3.6 µM); HeLa (IC ₅₀ = 2.9 µM); A-549 (IC ₅₀ = 3.2 µM)	<i>Aspergillus</i> sp. (ZA-01) isolated from sediment collected in the Bohai Sea	[45]
Aspergixanthone F (84)	MDA-MB-231 (IC ₅₀ = 9.8 µM); MCF-7 (IC ₅₀ = 2.7 µM); MGC-803 (IC ₅₀ = 3.6 µM); HeLa (IC ₅₀ = 1.7 µM); A-549 (IC ₅₀ = 1.1 µM)		
5-Methoxysterigmatocystin (85)	A-549 (IC ₅₀ = 3.86 µM); HL-60 (IC ₅₀ = 5.32 µM)	<i>Aspergillus versicolor</i>	[46]
Epiremispore B (121)	K562 (IC ₅₀ = 16.6 µM); MCF-7 (IC ₅₀ = 16.3 µM); SGC7901 (IC ₅₀ = 15.8 µM)	<i>Penicillium</i> sp. (SCSIO Ind16F01) isolated from a deep-sea sediment collected in the Indian Ocean	[47]
Dicerandrol C (122)	MDA-MB-435 (IC ₅₀ = 44.10 ± 2.45 µM); HCT-116 (IC ₅₀ = 42.63 ± 2.90 µM); Calu-3 (IC ₅₀ = 36.52 ± 3.32 µM); Huh7 (IC ₅₀ ≥ 50 µM); MCF-10A (IC ₅₀ = 33.05 ± 2.74 µM)	<i>Phomopsis</i> sp. (HNY29-2B) isolated from <i>Acanthus ilicifolius</i> collected in the South China Sea	[48]
Secalonic acid D (123)	PANC-1 Glucose (-) (IC ₅₀ = 0.6 µM); PANC-1 Glucose (+) (IC ₅₀ ≥ 1000 µM)	<i>Penicillium oxalicum</i> (16A08-1-1) isolated from a sponge collected at Pramuka Island	[49]
	U87 MG (IC ₅₀ = 5.64 µM); NCI-H1650 (IC ₅₀ = 4.93 µM); HT29 (IC ₅₀ = 1.46 µM); A498 (IC ₅₀ = 8.88 µM); HL-60 (IC ₅₀ = 0.41 µM)	<i>Penicillium chrysogenum</i> (HLS111) isolated from a sponge	[50]
	SK-HEP (IC ₅₀ = 1.504 µM); HeLa (IC ₅₀ = 1.322 µM); A549 (IC ₅₀ = 1.625 µM); SK-MES-1 (IC ₅₀ = 1.314 µM); SPC-A1 (IC ₅₀ = 1.679 µM); 95D (IC ₅₀ = 1.003 µM); Jeko-1 (IC ₅₀ = 0.915 µM); Raji (IC ₅₀ = 0.955 µM); U937 (IC ₅₀ = 1.119 µM); A375 (IC ₅₀ = 1.598 µM); HFF (IC ₅₀ = 24.1 µM); H22 (IC ₅₀ = 1.007 µM)	<i>Penicillium oxalicum</i> isolated from sediments collected on the southeast coastal region of China	[51]
Versixanthone G (124)	HL-60 (IC ₅₀ = 13.4 µM); K562 (IC ₅₀ = 20.9 µM); A549 (IC ₅₀ = 17.8 µM); H1975 (IC ₅₀ = 9.8 µM); MGC803 (IC ₅₀ = 4.6 µM); HEK293 (IC ₅₀ ≥ 50 µM); HO-8910 (IC ₅₀ = 9.6 µM); HCT-116 (IC ₅₀ = 16.2 µM)		
Versixanthone H (125)	HL-60 (IC ₅₀ = 6.9 µM); K562 (IC ₅₀ = 22.1 µM); A549 (IC ₅₀ = 19.2 µM); H1975 (IC ₅₀ = 5.3 µM); MGC803 (IC ₅₀ = 6.2 µM); HEK293 (IC ₅₀ ≥ 50 µM); HO-8910 (IC ₅₀ = 6.9 µM); HCT-116 (IC ₅₀ = 15.2 µM)		
Versixanthone I (126)	HL-60 (IC ₅₀ = 27.8 µM); K562 (IC ₅₀ ≥ 50.0 µM); A549 (IC ₅₀ ≥ 50.0 µM); H1975 (IC ₅₀ ≥ 50.0 µM); HEK293 (IC ₅₀ ≥ 50 µM); HO-8910 (IC ₅₀ ≥ 50.0 µM); HCT-116 (IC ₅₀ ≥ 50.0 µM)	<i>Aspergillus versicolor</i> isolated from mangrove	[52]
Versixanthone J (127)	HL-60 (IC ₅₀ = 47.3 µM); K562 (IC ₅₀ ≥ 50.0 µM); A549 (IC ₅₀ ≥ 50.0 µM); H1975 (IC ₅₀ ≥ 50.0 µM); HEK293 (IC ₅₀ ≥ 50 µM); HO-8910 (IC ₅₀ ≥ 50.0 µM); HCT-116 (IC ₅₀ ≥ 50.0 µM)		
Versixanthone K (128)	HL-60 (IC ₅₀ = 49.5 µM); K562 (IC ₅₀ ≥ 50.0 µM); A549 (IC ₅₀ ≥ 50.0 µM); H1975 (IC ₅₀ = 49.5 µM); MGC803 (IC ₅₀ ≥ 50.0 µM); HEK293 (IC ₅₀ ≥ 50 µM); HO-8910 (IC ₅₀ ≥ 50.0 µM); HCT-116 (IC ₅₀ ≥ 50.0 µM)		

Table 1. Cont.

Name	Activity	Source	Ref.
Versixanthone L (129)	HL-60 (IC ₅₀ = 0.5 µM); K562 (IC ₅₀ = 1.1 µM); A549 (IC ₅₀ = 1.6 µM); MGC803 (IC ₅₀ = 1.1 µM); HO-8910 (IC ₅₀ = 1.5 µM); HCT-116 (IC ₅₀ = 1.2 µM)	<i>Aspergillus versicolor</i> isolated from mangrove	[52]
Versixanthone M (130)	HL-60 (IC ₅₀ = 0.9 µM); K562 (IC ₅₀ = 0.4 µM); A549 (IC ₅₀ = 11.7 µM); H1975 (IC ₅₀ = 3.5 µM); MGC803 (IC ₅₀ = 0.9 µM); HO-8910 (IC ₅₀ = 1.4 µM); line HCT-116 (IC ₅₀ = 0.5 µM)		
Citreamicin ε A (131)	HeLa (IC ₅₀ = 0.032 ± 0.0062 µM); HepG2 (IC ₅₀ = 0.079 ± 0.031 µM)	<i>Streptomyces caelestis</i> collected on the coastal water of the Red Sea	[53]
Citreamicin ε B (132)	HeLa (IC ₅₀ = 0.031 ± 0.0081 µM); HepG2 (IC ₅₀ = 0.10 ± 0.0053 µM)		
Acredinone C (133)	Inhibited the RANKL- induced formation of TRAP ⁺ -MNCs in a dose-dependent manner without any cytotoxicity up to 10 µM	<i>Acremonium</i> sp. isolated from the inner tissue of <i>Suberites japonicas</i>	[54]
Phomolactonexanthone A (134)	Calu-3 (IC ₅₀ = 43.45 ± 2.51 µM)		
Deacetylphomoxanthone C (135)	HCT-116 (IC ₅₀ = 44.06 ± 3.29 µM); Calu-3 (IC ₅₀ = 43.35 ± 2.09 µM)		
Dicerandrol A (136)	MDA-MB-435 (IC ₅₀ = 3.03 ± 0.12 µM); HCT-116 (IC ₅₀ = 2.64 ± 0.03 µM); Calu-3 (IC ₅₀ = 1.76 ± 0.02 µM); Huh7 (IC ₅₀ = 4.19 ± 0.08 µM); MCF-10A (IC ₅₀ = 28.32 ± 3.57 µM)		
Dicerandrol B (137)	MDA-MB-435 (IC ₅₀ = 8.65 ± 0.66 µM); HCT-116 (IC ₅₀ = 3.94 ± 0.39 µM); Calu-3 (IC ₅₀ = 4.10 ± 0.08 µM); Huh7 (IC ₅₀ = 30.37 ± 1.10 µM); MCF-10A (IC ₅₀ = 8.14 ± 1.27 µM)	<i>Phomopsis</i> sp. (HNY29-2B) isolated from <i>Acanthus ilicifolius</i> collected in the South China Sea	[48]
Deacetylphomoxanthone B (138)	MDA-MB-435 (IC ₅₀ = 14.40 ± 1.18 µM); HCT-116 (IC ₅₀ = 7.12 ± 0.70 µM); Calu-3 (IC ₅₀ = 4.14 ± 0.02 µM); Huh7 (IC ₅₀ = 29.20 ± 1.19 µM)		
Penexanthone A (139)	MDA-MB-435 (IC ₅₀ = 7.90 ± 0.58 µM); HCT-116 (IC ₅₀ = 6.92 ± 0.38 µM); Calu-3 (IC ₅₀ = 6.44 ± 0.86 µM); Huh7 (IC ₅₀ = 42.82 ± 3.58 µM); MCF-10A (IC ₅₀ = 16.13 ± 1.57 µM)		
4,4'-bond Secalonic acid D (140)	SK- HEP (IC ₅₀ = 1.342 µM); HeLa (IC ₅₀ = 0.827 µM); A549 (IC ₅₀ = 1.353 µM); SK-MES-1 (IC ₅₀ = 0.640 µM); SPC-A1 (IC ₅₀ = 1.205 µM); 95D (IC ₅₀ = 0.978 µM); Jeko-1 (IC ₅₀ = 0.705 µM); Raji (IC ₅₀ = 0.484 µM); U937 (IC ₅₀ = 0.960 µM); A375 (IC ₅₀ = 1.085 µM); HFF (IC ₅₀ = 26.6 µM); H22 (IC ₅₀ = 1.211 µM)	<i>Penicillium oxalicum</i> isolated from sediments collected on the southeast coastal region of China	[51]
Phomoxanthone A (141)	HL-60 (cytotoxic at 0.1 to 0.01 µg mL ⁻¹)	<i>Phomopsis longicolla</i> isolated from <i>Bostrychia radicans</i>	[55]
JBIR-97 (142/143)	HeLa (IC ₅₀ = 11 µM); ACC-MESO-1 (IC ₅₀ = 31 µM)	<i>Tritirachium</i> sp. (SpB081112MEf2) isolated from <i>Pseudoceratina purpurea</i> collected at Ishigaki Island	[56]
JBIR-98 (142/143)	HeLa (IC ₅₀ = 17 µM); ACC-MESO-1 (IC ₅₀ = 63 µM)		
JBIR-99 (144)	HeLa (IC ₅₀ = 17 µM); ACC-MESO-1 (IC ₅₀ = 59 µM)		
Buanmycin (156)	A549 (IC ₅₀ = 1.7 µM); HCT116 (IC ₅₀ = 0.9 µM); SNU638 (IC ₅₀ = 0.8 µM); SK-HEP1 (IC ₅₀ = 1.9 µM); MDA-MB231 (IC ₅₀ = 1.2 µM)	<i>Streptomyces</i> sp. isolated from a tidal mudflat collected in Buan	[57]
	A549 (IC ₅₀ = 0.8 µM); HeLa (IC ₅₀ = 0.9 µM)	<i>Streptomyces</i> sp. (HGMA004) isolated from a mudflat collected at Uki	[58]

Table 1. Cont.

Name	Activity	Source	Ref.
Chrysoxanthone A (162)	U87 MG (IC ₅₀ = 22.6 μM); NCI-H1650 (IC ₅₀ = 42.2 μM); HT29 (IC ₅₀ = 41.8 μM); A498 (IC ₅₀ = 28.5 μM); HL-60 (IC ₅₀ = 37.2 μM)		
Chrysoxanthone B (163)	U87 MG (IC ₅₀ ≥ 50 μM); NCI-H1650 (IC ₅₀ ≥ 50 μM); HT29 (IC ₅₀ = 30.8 μM); A498 (IC ₅₀ ≥ 50 μM); HL-60 (IC ₅₀ = 16.2 μM)	<i>Penicillium chrysogenum</i> (HLS111) isolated from a sponge	[50]
Chrysoxanthone C (164)	U87 MG (IC ₅₀ = 47.0 μM); NCI-H1650 (IC ₅₀ ≥ 50 μM); HT29 (IC ₅₀ = 43.2 μM); A498 (IC ₅₀ ≥ 50 μM); HL-60 (IC ₅₀ = 22.7 μM)		
Ukixanthomycin A (165)	A549 (IC ₅₀ ≥ 200 μM); HeLa (IC ₅₀ ≥ 200 μM)	<i>Streptomyces</i> sp. (HGMA004) isolated from a mudflat collected at Uki	[58]

IC₅₀: half maximum inhibitory concentration; CD: concentration required to double quinone reductase activity.

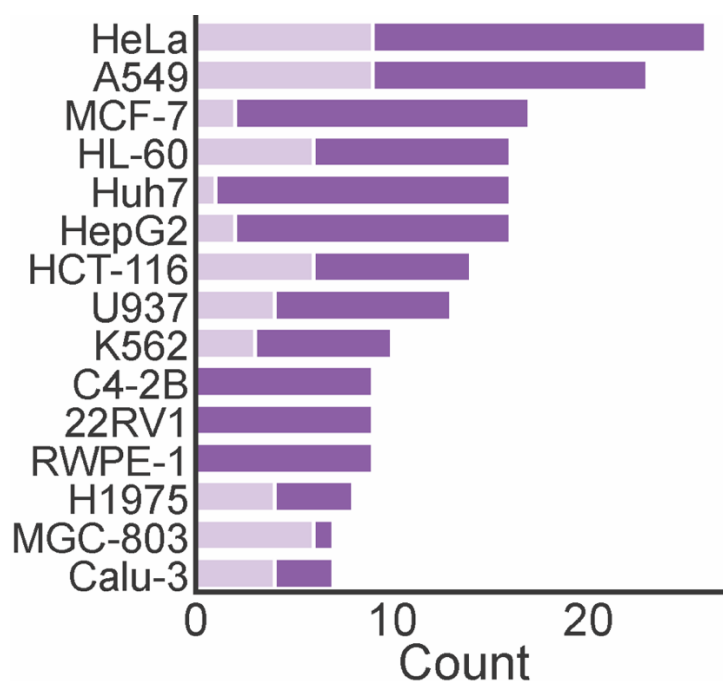


Figure 6. The number of antitumor marine xanthone and the most frequently assayed tumor cell lines. Dark purple bar represents the total count of the assayed xanthenes. Light purple bar represents the count of xanthenes with IC₅₀ lower than 10 μM.

A total of 54 marine xanthenes described in literature were evaluated for antibacterial activity, measuring the growth inhibitory activity of different bacteria (Table 2). Gram-positive bacteria were more exploited (144 assessments) than Gram-negative (78 assessments) (Figure 7a). The number of xanthenes with a minimum inhibitory concentration (MIC) lower than 4 μg mL⁻¹ varied depending on the tested bacteria. Marine xanthenes revealed a great selectivity for growth inhibition of Gram-positive bacteria as the percentage of marine xanthenes with MIC lower than 4 is significantly higher in these types of bacteria (28% Gram-positive vs. 8% Gram-negative). This could be ascribed to a target potentially involving the peptidoglycan layer that is present in Gram-positive bacteria and absent in Gram-negative bacteria. The majority of marine xanthenes were evaluated against *S. aureus* and *E. coli* (Figure 7b). Marine xanthenes were particularly active against *S. aureus*, *B. subtilis*, *E. faecalis*, which are all Gram-positive bacteria.

Table 2. Antibacterial marine xanthone.

Name	Activity	Source	Ref.
Sydowinin B (3)	<i>V. rotiferianus</i> (MCCC E385) (MIC = 32.6 ± 1.1 µg mL ⁻¹)	<i>Aspergillus sydowii</i> (C1-S01-A7) collected in the West Pacific Ocean	[32]
1,4,7-Trihydroxy-6-methylxanthone (15)	<i>E. coli</i> (MIC = 32 µg mL ⁻¹); <i>P. aeruginosa</i> (MIC = 32 µg mL ⁻¹); <i>S. aureus</i> (MIC > 64 µg mL ⁻¹); <i>V. alginolyticus</i> (MIC = 32 µg mL ⁻¹); <i>V. harveyi</i> (MIC = 32 µg mL ⁻¹); <i>V. parahaemolyticus</i> (MIC = 32 µg mL ⁻¹)	<i>Talaromyces islandicus</i> (EN-501) isolated from <i>Laurencia okamurai</i>	[59]
1,4,5-Trihydroxy-2-methylxanthone (16)	<i>E. coli</i> (MIC = 4 µg mL ⁻¹); <i>P. aeruginosa</i> (MIC = 4 µg mL ⁻¹); <i>S. aureus</i> (MIC = 8 µg mL ⁻¹); <i>V. alginolyticus</i> (MIC = 4 µg mL ⁻¹); <i>V. harveyi</i> (MIC = 8 µg mL ⁻¹); <i>V. parahaemolyticus</i> (MIC = 4 µg mL ⁻¹)		
Norlichexanthone (17)	<i>S. aureus</i> (ATCC 27154) (MIC = 12.5 µg mL ⁻¹); <i>E. coli</i> (ATCC 25922) (MIC > 100 µg mL ⁻¹); <i>S. ventriculi</i> (ATCC 29068) (MIC = 25.0 µg mL ⁻¹); <i>P. aeruginosa</i> (ATCC 25668) (MIC = 25.0 µg mL ⁻¹)	<i>Talaromyces</i> sp. (ZH-154) collected in the South China Sea	[60]
Yicathin C (18)	<i>E. coli</i> (zone of inhibition 12.0 mm); <i>S. aureus</i> (zone of inhibition 7.5 mm)	<i>Aspergillus wentii</i> isolated from <i>Gymnogongrus flabelliformis</i> collected at Pingtan Island	[61]
Yicathin B (19)	<i>E. coli</i> (zone of inhibition 9 mm)		
Fischexanthone (20)	<i>E. coli</i> (MIC > 1265.82 µM); <i>S. aureus</i> (MIC > 1265.82 µM)	<i>Alternaria</i> sp. (R6) isolated from mangrove collected at Leizhou peninsula	[62]
Methyl (2-chloro-1,6-dihydroxy-3-methylxanthone)-8-carboxylate (21)	<i>S. aureus</i> (ATCC43300) (MIC = 6.25 µg mL ⁻¹); <i>S. aureus</i> (ATCC29213) (MIC = 6.25 µg mL ⁻¹); <i>S. aureus</i> (ATCC33591) (MIC = 3.13 µg mL ⁻¹); <i>S. aureus</i> (ATCC25923) (MIC = 3.13 µg mL ⁻¹); <i>E. faecalis</i> (ATCC51299) (MIC = >100 µg mL ⁻¹); <i>E. faecium</i> (ATCC35667) (MIC = >100 µg mL ⁻¹); <i>V. parahaemolyticus</i> (ATCC17802) (MIC > 100 µg mL ⁻¹)	<i>Aspergillus flavipes</i> (DL-11) isolated from coastal sediment collected in Dalian	[63]
Methyl (4-chloro-1,6-dihydroxy-3-methylxanthone)-8-carboxylate (22)	<i>S. aureus</i> (ATCC43300) (MIC = 3.13 µg mL ⁻¹); <i>S. aureus</i> (ATCC29213) (MIC = 3.13 µg mL ⁻¹); <i>S. aureus</i> (ATCC33591) (MIC = 1.56 µg mL ⁻¹); <i>S. aureus</i> (ATCC25923) (MIC = 3.13 µg mL ⁻¹); <i>E. faecalis</i> (ATCC51299) (MIC 25 µg mL ⁻¹); <i>E. faecium</i> (ATCC35667) (MIC 50 µg mL ⁻¹); <i>V. parahaemolyticus</i> (ATCC17802) (MIC > 100 µg mL ⁻¹)		
2-Hydroxy-6-formyl-vertixanthone (23)	MRSA (ATCC 43300) (MIC = 16.3 ± 0.9 µg mL ⁻¹); MRSA (CGMCC 1.12409) (MIC = 16.1 ± 0.5 µg mL ⁻¹)		
12-O-Acetyl-sydowinin A (24)	MRSA (ATCC 43300) (MIC = 32.6 ± 0.8 µg mL ⁻¹); MRSA (CGMCC 1.12409) (MIC = 31.8 ± 0.8 µg mL ⁻¹)		
Emodin (25)	<i>V. vulnificus</i> (MCCC E1758) (MIC = 16.1 ± 0.7 µg mL ⁻¹); MRSA (ATCC 43300) (MIC = 15.4 ± 0.3 µg mL ⁻¹); MRSA (CGMCC 1.12409) (MIC = 15.7 ± 0.5 µg mL ⁻¹)	<i>Aspergillus sydowii</i> (C1-S01-A7) collected in the West Pacific Ocean	[32]
Aspergillusone A (26)	MRSA (ATCC 43300) (MIC = 32.2 ± 0.3 µg mL ⁻¹); MRSA (CGMCC 1.12409) (MIC = 32.4 ± 0.1 µg mL ⁻¹) BCG (<i>M. bovis</i> Pasteur 1173P2) (MIC = 20 µg mL ⁻¹)	<i>Aspergillus versicolor</i> (MF160003)	[64]
Chalaniline B (27)	Percent (%) growth of treated bacteria: <i>B. subtilis</i> (ATCC 49343) (67 ± 17%); <i>S. aureus</i> (ATCC 25923) (64 ± 14%); MRSA (ATCC BAA-41) (57 ± 8%); MRSA (ATCC BAA-44) (40 ± 2%)	Endophytic ascomycete with <i>Chalara</i> sp. (6661)	[65]
Engyodontiumone H (50)	<i>E. coli</i> (zone of inhibition 13.8 mm); <i>B. subtilis</i> (zone of inhibition 16.5 mm) <i>E. coli</i> (MIC = 64 µg mL ⁻¹); <i>B. subtilis</i> (MIC = 32 µg mL ⁻¹)	<i>Engyodontium album</i> (DFFS02) isolated from a sediment collected in the South China Sea	[28]
Aspergillusone B (63)	<i>E. coli</i> (zone of inhibition 11.0 mm); <i>B. subtilis</i> (zone of inhibition 14.4 mm) <i>E. coli</i> (MIC = 64 µg mL ⁻¹); <i>B. subtilis</i> (MIC = 64 µg mL ⁻¹)	<i>Engyodontium album</i> (DFFS02) isolated from a sediment collected in the South China Sea	

Table 2. Cont.

Name	Activity	Source	Ref.
AGI-B4 (64)	<i>E. coli</i> (zone of inhibition 15.8 mm); <i>B. subtilis</i> (zone of inhibition 17.5 mm)	<i>Engyodontium album</i> (DFFSCS02) isolated from sediment collected in the South China Sea	[28]
	<i>E. coli</i> (MIC = 64 µg mL ⁻¹); <i>B. subtilis</i> (MIC = 64 µg mL ⁻¹)	<i>Engyodontium album</i> (DFFSCS02) isolated from sediment collected in the South China Sea	
	<i>V. vulnificus</i> (MCCC E1758) (MIC = 32.5 ± 0.4 µg mL ⁻¹); MRSA (ATCC 43300) (MIC = 32.9 ± 0.3 µg mL ⁻¹); MRSA (CGMCC 1.12409) (MIC = 16.3 ± 0.5 µg mL ⁻¹)	Deep sea-derived fungus <i>Aspergillus sydowii</i> C1-S01-A7 isolated in the West Pacific Ocean	[32]
Blennolide A (65)	<i>E. coli</i> (zone of inhibition 7 mm); <i>B. megaterium</i> (zone of inhibition 8 mm)	<i>Blennoria</i> sp. isolated from <i>Carpobrotus edulis</i> collected at Gomera	[66]
Blennolide B (66)	<i>E. coli</i> (zone of inhibition 8 mm); <i>B. megaterium</i> (zone of inhibition 8 mm)		
Paeciloxanthone (68)	<i>E. coli</i> (zone of inhibition 12 mm)	<i>Paecilomyces</i> sp. isolated from a mangrove collected in the Taiwan Strait	[40]
Sterigmatocystin (81)	<i>S. aureus</i> (zone of inhibition 9.0 mm)	<i>Aspergillus versicolor</i>	[44]
Hemi-acetal sterigmatocystin (86)	<i>S. aureus</i> (ATCC 6538) (MIC > 100 µg mL ⁻¹); <i>B. subtilis</i> (ATCC 6633) (MIC > 100 µg mL ⁻¹); MRSA (MIC > 100 µg mL ⁻¹); <i>P. aeruginosa</i> (ATCC 15692) (MIC > 100 µg mL ⁻¹)	<i>Aspergillus versicolor</i> (MF359) isolated from <i>Hymeniacion perleve</i> collected in the Bohai Sea	[67]
Acyl-hemiacetal sterigmatocystin (87)	<i>S. aureus</i> (ATCC 6538) (MIC > 100 µg mL ⁻¹); <i>B. subtilis</i> (ATCC 6633) (MIC > 100 µg mL ⁻¹); MRSA (MIC > 100 µg/mL); <i>P. aeruginosa</i> (ATCC 15692) (MIC > 100 µg mL ⁻¹)		
5-Methoxydihydrosterigmatocystin (88)	<i>S. aureus</i> (ATCC 6538) (MIC = 12.5 µg mL ⁻¹); <i>B. subtilis</i> (ATCC 6633) (MIC = 3.125 µg mL ⁻¹); MRSA (MIC > 100 µg mL ⁻¹); <i>P. aeruginosa</i> (ATCC 15692) (MIC > 100 µg mL ⁻¹)		
Emerixanthone E (89)	<i>E. coli</i> (ATCC 29922); <i>K. pneumoniae</i> (ATCC 13883); <i>S. aureus</i> (ATCC 29213); <i>E. faecalis</i> (ATCC 29212); <i>A. baumannii</i> (ATCC 19606); <i>A. hydrophila</i> (ATCC 7966): Diameters of the inhibition zones ranged between 9 and 11 mm	<i>Emericella</i> sp. collected in the South China Sea	[68]
Emerixanthone A (90)	<i>E. coli</i> (ATCC 29922); <i>K. pneumoniae</i> (ATCC 13883); <i>S. aureus</i> (ATCC 29213); <i>E. faecalis</i> (ATCC 29212); <i>A. baumannii</i> (ATCC 19606); <i>A. hydrophila</i> (ATCC 7966): Diameters of inhibition zones were all 4–6 mm	<i>Emericella</i> sp. (SCSIO 05240) collected in the South China Sea	[69]
Emerixanthone C (91)	<i>E. coli</i> (ATCC 29922); <i>K. pneumoniae</i> (ATCC 13883); <i>S. aureus</i> (ATCC 29213); <i>E. faecalis</i> (ATCC 29212); <i>A. baumannii</i> (ATCC 19606); <i>A. hydrophila</i> (ATCC 7966): Diameters of inhibition zones were all 4–6 mm		
Varixanthone (92)	<i>E. coli</i> (MIC = 12.5 µg mL ⁻¹); <i>Proteus</i> sp. (MIC = 12.5 µg mL ⁻¹); <i>B. subtilis</i> (MIC = 12.5 µg mL ⁻¹); <i>S. aureus</i> (MIC = 12.5 µg mL ⁻¹); <i>E. faecalis</i> (MIC = 50 µg mL ⁻¹)	<i>Emericella varicolor</i> (M75-2) was isolated from a <i>Porifera</i> sp. collected in the Caribbean Sea	[70]
Oxisterigmatocystin C (93)	<i>S. aureus</i> (ATCC25923) (MIC < 48 µg mL ⁻¹)	<i>Aspergillus</i> sp. (F40) isolated from <i>Callyspongia</i> sp.	[71]
Aspergixanthone G (94)	<i>M. luteus</i> (MIC = 0.78 µg mL ⁻¹); <i>B. anthracis</i> (MIC = 12.5 µg mL ⁻¹); <i>S. typhi</i> (MIC = 6.13 µg mL ⁻¹); <i>E. aerogenes</i> (MIC = 6.13 µg mL ⁻¹)	<i>Aspergillus</i> sp. (ZA-01) isolated from sediment collected in the Bohai Sea	[45]
Aspergixanthone H (95)	<i>M. luteus</i> (MIC = 6.13 µg mL ⁻¹); <i>B. anthracis</i> (MIC = 12.5 µg mL ⁻¹); <i>S. typhi</i> (MIC = 6.13 µg mL ⁻¹); <i>E. aerogenes</i> (MIC = 6.13 µg mL ⁻¹)		
Dicerandrol C (122)	<i>S. aureus</i> (ATCC 6538) (MIC = 1.33 µM); <i>S. saprophyticus</i> (ATCC 15305) (MIC = 2.66 µM)	<i>Phomopsis longicolla</i> isolated from <i>Bostrychia radicans</i> collected in Brazil	[72]
Secalonic acid D (123)	<i>S. aureus</i> (ATCC 29,213) (IC ₅₀ = 7.19 µM); <i>M. tuberculosis</i> (IC ₅₀ = 1.26 µM)	<i>Aspergillus</i> sp. (SCSIO XWS03F03) isolated from a sponge	[73]
	<i>B. subtilis</i> (MIC = 24.4 µg mL ⁻¹); <i>E. coli</i> J(VC1228) (MIC = 24.4 µg mL ⁻¹); <i>M. luteus</i> (UST950701-006) (MIC = 24.4 µg mL ⁻¹); <i>P. nigrifaciens</i> (UST010620-005) (MIC = 97.5 µg mL ⁻¹)	<i>Penicillium</i> sp. (SCSGAF0023) isolated from <i>Dichotella gemmacea</i> collected in the South China Sea	[74]

Table 2. Cont.

Name	Activity	Source	Ref.
JBIR-97/98 (145)	<i>S. epidermidis</i> (IC ₅₀ = 0.20 ± 0.04 µM); MRSA (IC ₅₀ = 0.19 ± 0.02 µM); <i>P. acnes</i> (IC ₅₀ = 11.0 ± 1.3 µM)	<i>Engyodontium album</i> isolated from <i>Cacospinga scalaris</i> collected at the Limski Fjord	[75]
Engyodontochone A (146)	<i>S. epidermidis</i> (IC ₅₀ = 0.19 ± 0.04 µM); MRSA (IC ₅₀ = 0.17 ± 0.02 µM); <i>P. acnes</i> (IC ₅₀ = 13.8 ± 1.7 µM)		
JBIR-99 (147)	<i>S. epidermidis</i> (IC ₅₀ = 0.21 ± 0.09 µM); MRSA (IC ₅₀ = 0.25 ± 0.07 µM); <i>P. acnes</i> (IC ₅₀ = 14.1 ± 2.7 µM)		
Engyodontochone B (148)	<i>S. epidermidis</i> (IC ₅₀ = 0.22 ± 0.03 µM); MRSA (IC ₅₀ = 0.24 ± 0.04 µM); <i>P. acnes</i> (IC ₅₀ = 11.7 ± 2.4 µM)		
Microluside A (149)	<i>E. faecalis</i> (JH212) (MIC = 10 µM); <i>S. aureus</i> (NCTC 8325) (MIC = 13 µM)	<i>Micrococcus</i> sp. (EG45) isolated from <i>Sphaciospongia vagabunda</i> collected in the Red Sea	[76]
Citreamicin θ A (150)	<i>S. haemolyticus</i> (MIC = 0.5 µg mL ⁻¹); <i>S. aureus</i> (UST950701-005) (MIC = 1.0 µg mL ⁻¹); <i>B. subtilis</i> (769) (MIC = 0.25 µg mL ⁻¹); <i>S. aureus</i> (ATCC43300) (MIC = 0.25 µg mL ⁻¹)	<i>Streptomyces caelestis</i> collected in the Red Sea	[77]
Citreamicin θ B (151)	<i>S. haemolyticus</i> (UST950701-004) (MIC = 0.5 µg mL ⁻¹); <i>S. aureus</i> (UST950701-005) (MIC = 1.0 µg mL ⁻¹); <i>B. subtilis</i> (769) (MIC = 0.25 µg mL ⁻¹); <i>S. aureus</i> (ATCC43300) (MIC = 0.25 µg mL ⁻¹)		
Citreaglycon A (152)	<i>S. haemolyticus</i> (MIC = 8.0 µg mL ⁻¹); <i>S. aureus</i> (UST950701-005) (MIC = 16 µg mL ⁻¹); <i>B. subtilis</i> (769) (MIC = 8.0 µg mL ⁻¹); <i>S. aureus</i> (ATCC43300) (MIC = 8.0 µg mL ⁻¹)		
Dehydrocitreaglycon A (153)	<i>S. haemolyticus</i> (UST950701-004) (MIC = 8.0 µg mL ⁻¹); <i>S. aureus</i> (UST950701-005) (MIC = 16 µg mL ⁻¹); <i>B. subtilis</i> (769) (MIC = 8.0 µg mL ⁻¹)		
Penicillixanthone A (154)	<i>B. subtilis</i> (MIC = 24.4 µg mL ⁻¹); <i>E. coli</i> (JVC1228) (MIC = 24.4 µg mL ⁻¹); <i>M. luteus</i> (UST950701-006) (MIC = 24.4 µg mL ⁻¹); <i>P. nigrifaciens</i> (UST010620-005) (MIC = 97.5 µg mL ⁻¹)	<i>Penicillium</i> sp. (SCSGAF0023) isolated from <i>Dichotella gemmacea</i> collected in the South China Sea	[74]
IB-00208 (155)	<i>E. coli</i> (ATCC 10536) (MIC ≥ 150 nM); <i>K. pneumoniae</i> (ATCC 29665) (MIC ≥ 150 nM); <i>P. aeruginosa</i> (ATCC 10145) (MIC ≥ 150 nM); <i>B. subtilis</i> (ATCC 6051) (MIC = 1.4 nM); <i>S. aureus</i> (ATCC 6538P) (MIC = 1.4 nM); <i>M. luteus</i> (ATCC 9341) (MIC = 0.09 nM)	<i>Actinomadura</i> sp. collected at the northern coast of Spain	[78]
Buanmycin (156)	<i>S. aureus</i> (MIC = 10.5 µM, sortase A inhibition IC ₅₀ = 43.2 µM); <i>B. subtilis</i> (MIC = 0.7 µM); <i>K. rhizophila</i> (MIC = 10.5 µM); <i>S. enterica</i> (MIC = 0.7 µM); <i>P. hauseri</i> (MIC = 21.1 µM)	<i>Streptomyces</i> sp. isolated from a tidal mudflat collected in Buan	[57]
	<i>B. cereus</i> (IC ₅₀ = 3.0 µM); <i>E. coli</i> (IC ₅₀ = 6.0 µM)	<i>Streptomyces</i> sp. (HGMA004) isolated from a mudflat collected at Uki	[58]
Secalonic acid A (157)	<i>S. aureus</i> (ATCC 27154) (MIC = 12.5 µg mL ⁻¹); <i>E. coli</i> (ATCC 25922) (MIC = 25 µg mL ⁻¹); <i>S. ventriculi</i> (ATCC 29068) (MIC = 12.5 µg mL ⁻¹); <i>P. aeruginosa</i> (ATCC 25668) (MIC = 12.5 µg mL ⁻¹)	<i>Talaromyces</i> sp. (ZH-154) collected in the South China Sea	[60]
Secalonic acid B (158)	<i>B. subtilis</i> (MIC = 97.5 µg mL ⁻¹); <i>E. coli</i> (JVC1228) (MIC = 97.5 µg mL ⁻¹); <i>M. luteus</i> (UST950701-006) (MIC = 97.5 µg mL ⁻¹); <i>P. nigrifaciens</i> (UST010620-005) (MIC = 390.5 µg mL ⁻¹)	<i>Penicillium</i> sp. (SCSGAF0023) isolated from <i>Dichotella gemmacea</i> collected in the South China Sea	[74]
	<i>B. megaterium</i> (zone of inhibition 15 mm)	<i>Blennoria</i> sp. isolated from <i>Carpobrotus edulis</i> collected at Gomera	[66]

Table 2. Cont.

Name	Activity	Source	Ref.
Neocitreacin I (159)	<i>B. subtilis</i> 1A1 (MIC = 0.06 µg mL ⁻¹); <i>S. aureus</i> (MRSA NRS1) (MIC = 0.50 µg mL ⁻¹); <i>S. aureus</i> (MRSA NRS2) (MIC = 0.12 µg mL ⁻¹); <i>S. aureus</i> (MRSA NRS71) (MIC = 0.12 µg mL ⁻¹); <i>E. faecalis</i> (VRE 51299) (MIC = 0.06 µg mL ⁻¹); <i>E. faecalis</i> (VRE 51575) (MIC = 0.12 µg mL ⁻¹); <i>E. coli</i> K-12 (MIC ≥ 8.0 µg mL ⁻¹)	<i>Nocardia</i> sp. (G0655) isolated from a sandy soil sample collected in Falmouth	[79]
Neocitreacin II (160)	<i>B. subtilis</i> 1A1 (MIC = 0.12 µg mL ⁻¹); <i>S. aureus</i> (MRSA NRS1) (MIC = 1.0 µg mL ⁻¹); <i>S. aureus</i> (MRSA NRS2) (MIC = 0.50 µg mL ⁻¹); <i>S. aureus</i> (MRSA NRS71) (MIC = 0.50 µg mL ⁻¹); <i>E. faecalis</i> (VRE 51299) (MIC = 0.06 µg mL ⁻¹); <i>E. faecalis</i> (VRE 51575) (MIC = 0.25 µg mL ⁻¹); <i>E. coli</i> K-12 (MIC ≥ 8.0 µg mL ⁻¹)		
Citreacin α (161)	<i>E. coli</i> (MIC > 128 µg mL ⁻¹); <i>K. pneumoniae</i> (MIC > 128 µg mL ⁻¹); <i>Serratia</i> sp. (MIC > 128 µg mL ⁻¹); <i>Citrobacter</i> sp. (MIC > 128 µg mL ⁻¹); <i>P. aeruginosa</i> (MIC ≥ 128 µg mL ⁻¹); <i>S. aureus</i> (MIC < 0.06~0.12 µg mL ⁻¹); <i>S. epidermidis</i> (MIC < 0.06 µg mL ⁻¹); <i>Enterococcus</i> sp. (MIC < 0.06~0.12 µg mL ⁻¹); <i>Streptococcus</i> sp. (MIC < 0.06 µg mL ⁻¹); <i>S. pneumoniae</i> (MIC < 0.06 µg mL ⁻¹); <i>B. fragilis</i> (MIC = 16 µg mL ⁻¹); <i>B. thetaiotaomicron</i> (MIC = 4 µg mL ⁻¹); <i>Clostridium perfringens</i> (MIC < 0.06 µg mL ⁻¹); <i>C. difficile</i> (MIC < 0.06 µg mL ⁻¹)	Culture LL-E19085 was isolated from a soil sample collected at Lake Manyara	[80]
Chrysoxanthone A (162)	<i>B. subtilis</i> (ATCC 63501) (MIC = 5 µg mL ⁻¹); <i>E. coli</i> (ATCC 25922) (MIC > 100 µg mL ⁻¹)		
Chrysoxanthone B (163)	<i>S. epidermidis</i> (ATCC 12228, MSSE) (MIC = 10 µg mL ⁻¹); <i>S. aureus</i> (ATCC 29213, MSSA) (MIC = 20 µg mL ⁻¹); <i>B. subtilis</i> (ATCC 63501) (MIC = 5 µg mL ⁻¹); <i>E. faecalis</i> (ATCC 29212, VSE) (MIC ≥ 100 µg mL ⁻¹); <i>E. coli</i> (ATCC 25922) (MIC ≥ 100 µg mL ⁻¹)	<i>Penicillium chrysogenum</i> (HLS111) isolated from a sponge	[50]
Chrysoxanthone C (164)	<i>S. epidermidis</i> (ATCC 12228, MSSE) (MIC = 20 µg mL ⁻¹); <i>S. aureus</i> (ATCC 29213, MSSA) (MIC = 80 µg mL ⁻¹); <i>B. subtilis</i> (ATCC 63501) (MIC = 10 µg mL ⁻¹); <i>E. faecalis</i> (ATCC 29212, VSE) (MIC > 100 µg mL ⁻¹); <i>E. coli</i> (ATCC 25922) (MIC > 100 µg mL ⁻¹)		
Ukixanthomycin A (165)	<i>B. cereus</i> (IC ₅₀ > 200 µM); <i>E. coli</i> (IC ₅₀ > 200 µM)	<i>Streptomyces</i> sp. (HGMA004) isolated from a mudflat collected at Uki	[58]

MIC: Minimum inhibitory concentration, IC₅₀: Half maximal inhibitory concentration. *A. baumannii*: *Acinetobacter baumannii*; *A. hydrophila*: *Aeromonas hydrophila*; *B. anthracis*: *Bacillus anthracis*; *B. cereus*: *Bacillus cereus*; *B. fragilis*: *Bacteroides fragilis*; *B. megaterium*: *Bacillus megaterium*; *B. subtilis*: *Bacillus subtilis*; *B. thetaiotaomicron*: *Bacteroides thetaiotaomicron*; *C. difficile*: *Clostridium difficile*; *C. perfringens*: *Clostridium perfringens*; *E. coli*: *Escherichia coli*; *E. aerogenes*: *Enterobacter aerogenes*; *E. faecalis*: *Enterococcus faecalis*; *E. faecium*: *Enterococcus faecium*; *K. pneumoniae*: *Klebsiella pneumoniae*; *K. rhizophila*: *Kocuria rhizophila*; *M. bovis*: *Mycobacterium bovis*; *M. luteus*: *Micrococcus luteus*; *M. tuberculosis*: *Mycobacterium tuberculosis*; MRSA: Methicillin-resistant *Staphylococcus aureus*; *P. acnes*: *Propionibacterium acnes*; *P. aeruginosa*: *Pseudomonas aeruginosa*; *P. hauseri*: *Proteus hauseri*; *P. nigrifaciens*: *Pseudoalteromonas nigrifaciens*; *S. aureus*: *Staphylococcus aureus*; *S. enterica*: *Salmonella enterica*; *S. epidermidis*: *Staphylococcus epidermidis*; *S. haemolyticus*: *Staphylococcus haemolyticus*; *S. pneumoniae*: *Streptococcus pneumoniae*; *S. saprophyticus*: *Staphylococcus saprophyticus*; *S. typhi*: *Salmonella typhi*; *S. ventriculi*: *Sarcina ventriculi*; *V. alginolyticus*: *Vibrio alginolyticus*; *V. harveyi*: *Vibrio harveyi*; *V. parahaemolyticus*: *Vibrio parahaemolyticus*; *V. rotiferianus*: *Vibrio rotiferianus*; *V. vulnificus*: *Vibrio vulnificus*.

A total of 21 marine xanthenes were evaluated for the antifungal activity against 17 different fungi, measuring the growth inhibitory activity of different fungi (Table 3). Among the evaluated fungi, *Fusarium* (12 xanthenes), *Colletotrichum* (8 xanthenes), *Candida* (5 xanthenes), and *Microbotryum* (4 xanthenes) were the most frequent genus.

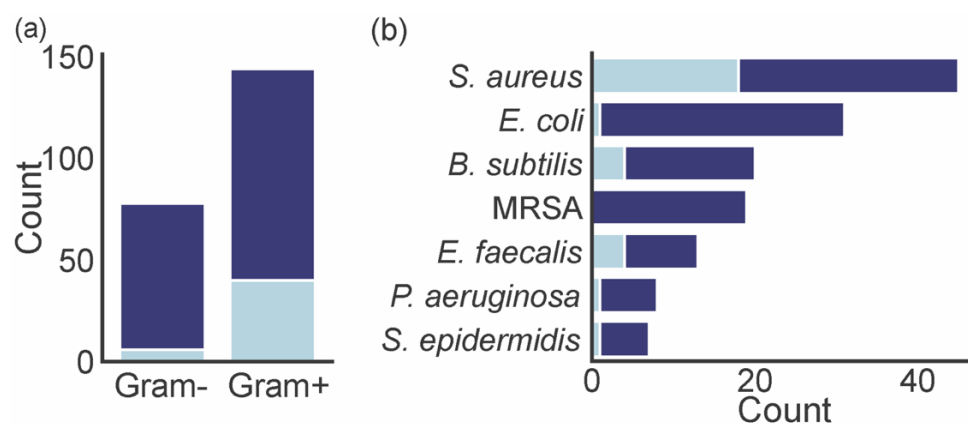


Figure 7. (a) The number of antibacterial marine xanthenes evaluated against Gram-positive and Gram-negative bacteria. Dark blue bar represents the total count of the assayed xanthenes. Light blue bar represents the count of xanthenes with MIC lower than $4 \mu\text{g mL}^{-1}$. (b) The bacteria that were assayed for antibacterial activity. Dark blue bar represents the total count of the assayed xanthenes. Light blue bar represents the count of xanthenes with MIC lower than $4 \mu\text{g mL}^{-1}$.

Table 3. Antifungal marine xanthone.

Name	Activity	Source	Ref.
Norlichexanthone (17)	<i>B. megaterium</i> (zone of inhibition 1 mm)	<i>Enteromorpha</i> sp. collected at Fehmarn Island	[81]
	<i>C. albicans</i> (ATCC 10231) (MIC = $6.25 \mu\text{g mL}^{-1}$); <i>A. niger</i> (ATCC 13496) (MIC = $25.0 \mu\text{g mL}^{-1}$); <i>F. oxysporum</i> f. sp. <i>cubense</i> (MIC = $50.0 \mu\text{g mL}^{-1}$)	<i>Talaromyces</i> sp. (ZH-154) collected in the South China Sea	[60]
Yicathin C (18)	<i>C. lagenarium</i> (zone of inhibition 11.0 mm)	<i>Aspergillus wentii</i> isolated from <i>Gymnogongrus flabelliformis</i> collected at Pingtan Island	[61]
Fischexanthone (20)	<i>F. graminearum</i> (MIC = $474.68 \mu\text{M}$); <i>C. musae</i> (MIC = $474.68 \mu\text{M}$)	<i>Alternaria</i> sp. (R6) isolated from mangrove collected at Leizhou peninsula	[62]
2,3,6,8-Tetrahydroxy-1-methylxanthone (28)	<i>M. violaceum</i> (zone of inhibition 1 mm)	<i>Enteromorpha</i> sp. collected at Fehmarn Island	[81]
Dimethyl 8-methoxy-9-oxo-9H-xanthene-1, 6-dicarboxylate (29)	<i>F. oxysporum</i> f. sp. <i>cubense</i> (MIC = $12.5 \mu\text{g mL}^{-1}$)	<i>Penicillium</i> sp. ZZF 32# collected in the South China Sea	[82,83]
1-Hydroxy-6-methyl-8-(hydroxymethyl)xanthone (30)	<i>E. repens</i> (zone of inhibition 2 mm) <i>U. violacea</i> (zone of inhibition 2 mm)	<i>Ulocladium botrytis</i> (193A4) isolated from the <i>Callispongia vaginalis</i> collected at Dominica	[84]
4-Chlorofischexanthone (31)	<i>F. graminearum</i> (MIC = $107 \mu\text{M}$) <i>C. musae</i> (MIC = $214 \mu\text{M}$)	<i>Alternaria</i> sp. (R6) isolated from mangrove collected at Leizhou peninsula	[62]
8-Hydroxy-3-methyl-9-oxo-9H-xanthene-1-carboxylic acid methyl ether (32)	<i>G. musae</i> (Rate of inhibition 53%); <i>P. cichoralearum</i> (Rate of inhibition 48%); <i>C. gloeosporioides</i> (Rate of inhibition 28%); <i>B. graminearum</i> (Rate of inhibition 4.6%); <i>F. oxysporum</i> (Rate of inhibition 9.5%)	Co-culture broth of mangrove fungi (strain No. K38 and E33) collected in the South China Sea	[85,86]
Globosuxanthone A (56)	<i>C. albicans</i> IFM 4954 (zone of inhibition 7 mm)	<i>Beauveria bassiana</i> (TPU942) isolated from a sponge collected at Iriomote Island	[35]
Blennolide A (65)	<i>M. violaceum</i> (zone of inhibition 9 mm)	<i>Blennoria</i> sp. isolated from <i>Carpobrotus edulis</i> collected at Gomera	[66]
Blennolide B (66)	<i>M. violaceum</i> (zone of inhibition 8 mm)		
Paeciloxanthone (68)	<i>C. lunata</i> (zone of inhibition 6 mm); <i>C. albicans</i> (zone of inhibition 10 mm)	<i>Paecilomyces</i> sp. isolated from a mangrove collected in the Taiwan Strait	[40]

Table 3. Cont.

Name	Activity	Source	Ref.
Versicone A (74)	<i>C. acutatum</i> (MIC = 32 µg mL ⁻¹); <i>F. oxysporum</i> (MIC = 128 µg mL ⁻¹); <i>M. oryzae</i> (MIC > 200 µg mL ⁻¹)		
Versicone B (75)	<i>C. acutatum</i> (MIC > 200 µg mL ⁻¹); <i>F. oxysporum</i> (MIC > 200 µg mL ⁻¹); <i>M. oryzae</i> (MIC > 200 µg mL ⁻¹)		
Versicone C (76)	<i>C. acutatum</i> (MIC > 200 µg mL ⁻¹); <i>F. oxysporum</i> (MIC > 200 µg mL ⁻¹); <i>M. oryzae</i> (MIC > 200 µg mL ⁻¹)	<i>Aspergillus versicolor</i> (SCSIO 05879) collected in the Indian Ocean	[87]
Versicone D (77)	<i>C. acutatum</i> (MIC > 200 µg mL ⁻¹); <i>F. oxysporum</i> (MIC > 200 µg mL ⁻¹); <i>M. oryzae</i> (MIC > 200 µg mL ⁻¹)		
Emerixanthone D (109)	<i>Fusarium</i> sp., <i>Penicillium</i> sp., <i>A. niger</i> , <i>R. solani</i> , <i>F. oxysporum</i> f. sp. <i>niveum</i> , <i>F. oxysporum</i> f. sp. <i>cucumeris</i> : Diameters of inhibition zones of which were both 3–4 mm	<i>Emericella</i> sp. (SCSIO 05240) collected in the South China Sea	[69]
Buanmycin (156)	<i>C. albicans</i> (MIC = 21.1 µM); <i>A. fumigatus</i> (MIC = 84.3 µM)	<i>Streptomyces</i> sp. isolated from a tidal mudflat collected in Buan	[57]
	<i>C. albicans</i> (IC ₅₀ = 0.4 µM)	<i>Streptomyces</i> sp. (HGMA004) isolated from a mudflat collected at Uki	[58]
Secalonic acid A (157)	<i>C. albicans</i> (ATCC 10231) (MIC = 6.25 µg mL ⁻¹); <i>A. niger</i> (ATCC 13496) (MIC = 6.25 µg mL ⁻¹); <i>F. oxysporum</i> f. sp. <i>cubense</i> (MIC = 12.5 µg mL ⁻¹)	<i>Talaromyces</i> sp. (ZH-154) collected in the South China Sea	[60]
Secalonic acid B (158)	<i>M. violaceum</i> (zone of inhibition 13 mm)	<i>Blennoria</i> sp. isolated from <i>Carpobrotus edulis</i> collected at Gomera	[66]
Ukixanthomycin A (165)	<i>C. albicans</i> (IC ₅₀ = 11.5 µM)	<i>Streptomyces</i> sp. (HGMA004) isolated from a mudflat collected at Uki	[58]

MIC: Minimum inhibitory concentration, IC₅₀: Half maximal inhibitory concentration. *A. fumigatus*: *Aspergillus fumigatus*; *A. niger*: *Aspergillus niger*; *C. albicans*: *Candida albicans*; *C. acutatum*: *Colletotrichum acutatum*; *C. gloeosporioides*: *Colletotrichum gloeosporioides*; *C. lagenarium*: *Colletotrichum lagenarium*; *C. lunata*: *Curvularia lunata*; *C. musae*: *Colletotrichum musae*; *E. repens*: *Eurotium repens*; *F. graminearum*: *Fusarium graminearum*; *F. oxysporum*: *Fusarium oxysporum*; *G. musae*: *Gloeosporium musae*; *M. oryzae*: *Magnaporthe oryzae*; *M. violaceum*: *Microbotryum violaceum*; *P. cichoralearum*: *Peronophthora cichoralearum*; *R. solani*: *Rhizoctonia solani*; *U. violacea*: *Ustilago violacea*.

A total of 18 marine xanthenes were evaluated against different viral targets of H1N1 (10 xanthenes), HSV-2 (10 xanthenes), HSV-1 (7 xanthenes), HIV-1 (3 xanthenes), EV71 (2 xanthenes), H3N2 (2 xanthenes), TMV (1 xanthone) (Table 4).

Table 4. Antiviral marine xanthone.

Name	Activity	Source	Ref.
Norlichexanthone (17)	EV71 (IC ₅₀ = 40.3 µM)	<i>Stachybotry</i> sp. (ZSDS1F1-2) isolated from a sponge collected at Xisha Island	[34]
2,3,6,8-Tetrahydroxy-1-methylxanthone (28)	HIV-1-RT (82.9% inhibition at 66 µg mL ⁻¹)		
	HIV-1-RT (82.2% inhibition at 66 µg mL ⁻¹)	<i>Enteromorpha</i> sp. collected at Fehmarn Island	[81]
3,8-Dihydroxy-6-methyl-9-oxo-9H-xanthene-1-carboxylate (33)	H1N1 (A/Puerto Rico/8/34 H274Y) (IC ₅₀ = 9.40 ± 1.96 µM); H1N1 (A/FM-1/1/47) (IC ₅₀ = 4.80 ± 1.28 µM); H3N2 (A/Aichi/2/68) (IC ₅₀ = 5.12 ± 1.49 µM)	<i>Diaporthe</i> sp. (SCSIO 41011), isolated from <i>Rhizophora stylosa</i>	[88]

Table 4. Cont.

Name	Activity	Source	Ref.
Methyl-(2-chloro-1,6-dihydroxy-3-methylxanthone)-8-carboxylate (34)	H1N1 (IC ₅₀ = 133.4 μM); HSV-1 (IC ₅₀ = 55.5 μM); HSV-2 (IC ₅₀ = 175.5 μM)		
Methyl-(4-chloro-1,6-dihydroxy-3-methylxanthone)-8-carboxylate (35)	H1N1 (IC ₅₀ = 44.6 μM); HSV-1 (IC ₅₀ = 21.4 μM); HSV-2 (IC ₅₀ = 76.7 μM)		
Methyl-(4-chloro-6-hydroxy-1-methoxy-3-methylxanthone)-8-carboxylate (36)	H1N1 (IC ₅₀ ≥ 200 μM); HSV-1 (IC ₅₀ = 139.4 μM); HSV-2 (IC ₅₀ ≥ 200 μM)		
Methyl-(6-hydroxy-1-methoxy-3-methylxanthone)-8-carboxylate (37)	H1N1 (IC ₅₀ ≥ 200 μM); HSV-1 (IC ₅₀ = 157.7 μM); HSV-2 (IC ₅₀ = 163.3 μM)	<i>Aspergillus iizukae</i> collected from coastal saline soil	[89]
4-Chloro-1,6-dihydroxy-3-methylxanthone-8-carboxylic acid (38)	H1N1 (IC ₅₀ ≥ 200 μM); HSV-1 (IC ₅₀ = 183.3 μM); HSV-2 (IC ₅₀ ≥ 200 μM)		
2,4-Dichloro-1,6-dihydroxy-3-methylxanthone-8-carboxylic acid (39)	H1N1 (IC ₅₀ ≥ 200 μM); HSV-1 (IC ₅₀ = 144.4 μM); HSV-2 (IC ₅₀ ≥ 200 μM)		
Methyl-(1,6-dihydroxy-3-methylxanthone)-8-carboxylate (40)	H1N1 (IC ₅₀ = 140.4 μM); HSV-1 (IC ₅₀ = 75.7 μM); HSV-2 (IC ₅₀ = 95.4 μM)		
2-Hydroxy-1-(hydroxymethyl)-8-methoxy-3-methyl-9H-xanthen-9-one (41)	H1N1 (A/PuertoRico/8/34) (IC ₅₀ = 4.70 ± 1.11 μM); H1N1 (A/FM-1/1/47) (IC ₅₀ = 4.04 ± 0.58 μM)	<i>Aspergillus sydowii</i> (SCSIO 41.301) isolated from <i>Phakellia fusca</i>	[90]
2-Hydroxy-1-(hydroxymethyl)-7,8-dimethoxy-3-methyl-9H-xanthen-9-one (42)	H1N1 (A/PuertoRico/8/34) (IC ₅₀ = 2.17 ± 1.39 μM)		
Sterigmatocystin A (110)	HSV-2 (IC ₅₀ = 47.11 μM)	<i>Aspergillus versicolor</i> (15XS43ZD-1) strain was isolated from sponge collected from Xisha Islands, China	[91]
Sterigmatocystin B (111)	HSV-2 (IC ₅₀ = 39.45 μM)		
Sterigmatocystin C (112)	HSV-2 (IC ₅₀ = 38.73 μM)		
Asperxanthone (113)	Tobacco mosaic virus: inhibitory rate 62.9%	<i>Aspergillus</i> sp. collected in Quan-Zhou Gulf	[92]
Epiremispore B (121)	EV71 (IC ₅₀ = 19.8 μM); H3N2 (IC ₅₀ = 24.1 μM)	<i>Penicillium</i> sp. (SCSIO Ind16F01) isolated from sediment collected in the Indian Ocean	[47]
Penicillixanthone A (154)	HIV-1 (SF162) (10 μM, 90.86 ± 0.82%); HIV-1 (CCR5-tropic) (IC ₅₀ = 0.36 μM); HIV-1 (CXCR4-tropic) (IC ₅₀ = 0.26 μM)	<i>Aspergillus fumigates</i> isolated from a jellyfish	[93]

EV71: Enterovirus 71; H1N1: Influenza A virus subtype H1N1; H3N2: Influenza A virus subtype H3N2; HIV: human immunodeficiency virus; HSV: herpes simplex virus; IC₅₀: Half maximal inhibitory concentration; RT: Reverse-transcriptase.

A total of 19 marine xanthenes were evaluated for antidiabetic activity using two different approaches: the assessment of α -glucosidase or protein tyrosine phosphatases inhibition activity and the assessment of the induction of the pancreatic β -cells proliferation in a zea fish model (Table 5).

A total of 9 marine xanthenes were evaluated for anti-oxidant activity through the DPPH assay and ABTS or trolox equivalent antioxidant capacity (TEAC) assay (Table 6).

A total of 8 marine xanthenes were evaluated for anti-inflammatory activity by measuring the inhibitory activity against cyclooxygenase (COX), by measuring the inhibition of inflammatory response induced by nitric oxide (NO) and NF- κ B (factor nuclear kappa B), and by measuring the decrease in IL-6 cytokine production on LPS-stimulated macrophages (Table 7).

Table 5. Antidiabetic marine xanthone.

Name	Activity	Source	Ref.
Chrysoxanthone (48)	α -Glucosidase inhibition (IC ₅₀ = 0.04 mM)	<i>Penicillium chrysogenum</i> (SCSIO 41001) isolated from sediment collected in the Indian Ocean	[94]
Staprexanthone A (69)	Pancreatic β -cell number (zebrafish model): ~40 at 10 μ M	<i>Stachybotrys chartarum</i> (HDN16-358) isolated from mangrove collected in Fujian Province	[95]
Staprexanthone B (70)	Pancreatic β -cell number (zebrafish model): 40 at 10 μ M		
Staprexanthone C (71)	Pancreatic β -cell number (zebrafish model): ~35 at 10 μ M		
Staprexanthone D (72)	Pancreatic β -cell number (zebrafish model): ~35 at 10 μ M		
Staprexanthone E (73)	Pancreatic β -cell number (zebrafish model): ~40 at 10 μ M		
Austocystin J (96)	Inhibitory effect against phosphatases: SHP1 (IC ₅₀ = 15 μ M); MEG2 (IC ₅₀ = 77 μ M)	<i>Aspergillus puniceus</i> (SCSIO z021)	[96]
Austocystin K (97)	Inhibitory effect against phosphatases: TCPTP (IC ₅₀ = 16 μ M); SHP1 (IC ₅₀ = 3.8 μ M)		
Austocystin L (98)	Inhibitory effect against phosphatases: TCPTP (IC ₅₀ = 12 μ M); SHP1 (IC ₅₀ = 20 μ M); CDC25B (IC ₅₀ = 24 μ M)		
Austocystin M (99)	Inhibitory effect against phosphatases: TCPTP (IC ₅₀ = 12 μ M); SHP2 (IC ₅₀ = 9.5 μ M); PTP1B (IC ₅₀ = 4.6 μ M)		
Austocystin N (100)	Inhibitory effect against phosphatases: SHP1 (IC ₅₀ = 17 μ M)		
Austocystin I (101)	Inhibitory effect against phosphatases: MEG2 (IC ₅₀ = 16 μ M); CDC25B (IC ₅₀ = 19 μ M)		
Austocystin F (102)	Inhibitory effect against phosphatases: SHP1 (IC ₅₀ = 6.7 μ M); MEG2 (IC ₅₀ = 2.1 μ M); CDC25B (IC ₅₀ = 6.7 μ M); CD45 (IC ₅₀ = 20 μ M)		
Austocystin A (103)	Inhibitory effect against phosphatases: TCPTP (IC ₅₀ = 19 μ M); MEG2 (IC ₅₀ = 8.1 μ M); CDC25B (IC ₅₀ = 16 μ M)		
Austocystin H (104)	Inhibitory effect against phosphatases: TCPTP (IC ₅₀ = 3.0 μ M); SHP1 (IC ₅₀ = 1.3 μ M); SHP2 (IC ₅₀ = 1.3 μ M); MEG2 (IC ₅₀ = 0.60 μ M); PTP1B (IC ₅₀ = 0.90 μ M); CDC25B (IC ₅₀ = 1.3 μ M); CD45 (IC ₅₀ = 14 μ M)		
Austocystin B (105)	Inhibitory effect against phosphatases: TCPTP (IC ₅₀ = 8.8 μ M); SHP2 (IC ₅₀ = 2.0 μ M); MEG2 (IC ₅₀ = 1.3 μ M); PTP1B (IC ₅₀ = 1.8 μ M); CDC25B (IC ₅₀ = 1.3 μ M)		
Austocystin D (106)	Inhibitory effect against phosphatases: PTP1B (IC ₅₀ = 1.7 μ M)		
8-O-Methyldihydrodemethylsterigmatocystin (107)	Inhibitory effect against phosphatases: TCPTP (IC ₅₀ = 11 μ M); SHP1 (IC ₅₀ = 5.5 μ M); MEG2 (IC ₅₀ = 4.6 μ M); CDC25B (IC ₅₀ = 4.9 μ M); CD45 (IC ₅₀ = 6.1 μ M)		
(1' R,2' R)-compound V (108)	Inhibitory effect against phosphatases: TCPTP (IC ₅₀ = 19 μ M); SHP1 (IC ₅₀ = 6.9 μ M); MEG2 (IC ₅₀ = 4.2 μ M)		

IC₅₀: Half maximal inhibitory concentration.

Table 6. Antioxidant marine xanthone.

Name	Activity	Source	Ref.
1,4,7-Trihydroxy-6-methylxanthone (15)	DPPH (IC ₅₀ = 6.92 µg mL ⁻¹); ABTS (IC ₅₀ = 2.35 µg mL ⁻¹)	<i>Talaromyces islandicus</i> (EN-501) isolated from <i>Laurencia okamurai</i>	[59]
1,4,5-Trihydroxy-2-methylxanthone (16)	DPPH (IC ₅₀ = 1.23 µg mL ⁻¹); ABTS (IC ₅₀ = 1.27 µg mL ⁻¹)		
Norlichexanthone (17)	DPPH (% Scavenging effect: 6.2% at 25.0 µg mL ⁻¹ ; 12.9% at 50 µg mL ⁻¹ ; 25.3% at 100 µg mL ⁻¹ ; 90.6% at 500 µg mL ⁻¹)		
2,3,6,8-Tetrahydroxy-1-methylxanthone (28)	DPPH (% Scavenging effect: 94.7% at 25.0 µg mL ⁻¹ ; 94.8% at 50 µg mL ⁻¹ ; 95.2% at 100 µg mL ⁻¹ ; 95.4% at 500 µg mL ⁻¹) Linolenic acid peroxidation (% Inhibition: 17.0% at 7.4 µg mL ⁻¹ ; 37.0% at 37 µg mL ⁻¹)	<i>Enteromorpha</i> sp. collected at Fehmarn Island	[81]
Arthone C (43)	DPPH (IC ₅₀ = 16.9 µM); ABTS (IC ₅₀ = 18.7 µM)		
2,3,4,6,8-Pentahydroxy-1-methylxanthone (44)	DPPH (IC ₅₀ = 22.1 µM); ABTS (IC ₅₀ = 18.0 µM)	<i>Arthrinium</i> sp. (UJNMF0008)	[97]
Sterigmatocystin (81)	ABTS (0.65 ± 0.13 TEAC values)	<i>Aspergillus versicolor</i> (A-21-2-7) isolated from sediment collected in the South China Sea	[98]
Oxisterigmatocystin C (93)	ABTS (1.16 ± 0.18 TEAC values)		
Oxisterigmatocystin D (120)	ABTS (0.55 ± 0.13 TEAC values)		

ABTS: (2,2'-azino-bis(3-ethylbenzothiazoline-6-sulfonic acid)); DPPH: (2,2-diphenyl-1-picryl-hydrazyl-hydrate); IC₅₀: Half maximal inhibitory concentration; TEAC: Trolox equivalents antioxidant capacity.

Table 7. Anti-inflammatory marine xanthone.

Name	Activity	Source	Ref.
Norlichexanthone (17)	COX-2 (IC ₅₀ = 34.3 µM)	<i>Stachybotry</i> sp. (ZSDS1F1-2) isolated from a sponge collected at Xisha Island	[34]
Yicathin C (18)	NO inhibition (27.0 ± 3.2%); NF-κB inhibition (56.8 ± 5.7%)	<i>Aspergillus europaeus</i> (WZXY-SX-4-1) isolated from <i>Xestospongia testudinaria</i>	[99]
Yicathin B (19)	IL-6 cytokine % at 1 µM: 78.37 ± 7.78%	<i>Aspergillus wentii</i> isolated from <i>Gymnogongrus flabelliformis</i> collected at Pingtan Island	[4]
	IL-6 cytokine % at 10 µM: 95.65 ± 17.21%		
	NO inhibition (35.3 ± 3.9%); NF-κB inhibition (81.2 ± 8.3%)	<i>Aspergillus europaeus</i> (WZXY-SX-4-1) isolated from <i>Xestospongia testudinaria</i>	[99]
1,3,6-trihydroxy-8-methylxanthone (45)	COX-2 (IC ₅₀ = 12.2 µM)	<i>Arthrinium</i> sp. (ZSDS1-F3) isolated from a sponge collected at Xisha Islands	[100]

Table 7. Cont.

Name	Activity	Source	Ref.
Calyxanthone (46)	NO inhibition (17.6 ± 5.1) NF- κ B: 63.7 ± 5.6		
Yicathin A (47)	NO inhibition ($23.7 \pm 4.8\%$); NF- κ B inhibition ($13.0 \pm 9.8\%$)	<i>Aspergillus europaeus</i> (WZXY-SX-4-1) isolated from <i>Xestospongia testudinaria</i>	[99]
Euroanthone A (166)	NO inhibition ($42.2 \pm 2.3\%$); NF- κ B inhibition ($68.8 \pm 7.0\%$)		
Euroanthone B (167)	NO inhibition ($23.4 \pm 3.3\%$); NF- κ B inhibition ($52.3 \pm 10.6\%$)		

COX: Cyclooxygenase; IC₅₀: Half maximal inhibitory concentration; NF- κ B: factor nuclear kappa B; NO: nitric oxide.

The remaining biological activities were classified as miscellaneous (Table 8). Seven marine xanthenes were evaluated for their immunosuppressive activity through the assessment of the inhibition of proliferation of mouse splenic lymphocytes stimulated with Con-A and LPS. One xanthone was evaluated for its anti-Alzheimer activity through the assessment of acetylcholinesterase inhibition. Three marine xanthenes were evaluated for their anti-protozoal activity against *Trypanosoma brucei*, *Trypanosoma cruzi*, *Leshmania donovani*, and *Plamodium falciparum*. Nine marine xanthenes were evaluated for their aquatic pathogens biocide activity against *Vibrio* sp.

Table 8. Marine xanthone with miscellaneous biological activities.

Name	Activity	Source	Ref.
Sydowinin A (2)	Immunosuppressive: Inhibition of Con A-Induced proliferation (IC ₅₀ = $6.5 \mu\text{g mL}^{-1}$); Inhibition of LPS-Induced proliferation (IC ₅₀ = $7.1 \mu\text{g mL}^{-1}$)		
Sydowinin B (3)	Immunosuppressive: Inhibition of Con A-Induced proliferation (IC ₅₀ = $19.2 \mu\text{g mL}^{-1}$); Inhibition of LPS-Induced proliferation (IC ₅₀ = $20.8 \mu\text{g mL}^{-1}$)		
Methyl 8-hydroxy-6-methyl-9-oxo-9H-xanthene-1- carboxylate (7)	Immunosuppressive: Inhibition of Con A-Induced proliferation (IC ₅₀ = $25.7 \mu\text{g mL}^{-1}$); Inhibition of LPS-Induced proliferation (IC ₅₀ = $26.4 \mu\text{g mL}^{-1}$)		
Conioxanthone A (12)	Immunosuppressive: Inhibition of Con A-Induced proliferation (IC ₅₀ = $8.2 \mu\text{g mL}^{-1}$); Inhibition of LPS-Induced proliferation (IC ₅₀ = $7.5 \mu\text{g mL}^{-1}$)	<i>Penicillium</i> sp. (ZJ-SY2) isolated from <i>Sonneratia apetala</i>	[101]
Pinselins (49)	Immunosuppressive: Inhibition of Con A-Induced proliferation (IC ₅₀ = $5.9 \mu\text{g mL}^{-1}$); Inhibition of LPS-Induced proliferation (IC ₅₀ = $7.5 \mu\text{g mL}^{-1}$)		
Epiremisporsine B (121)	Immunosuppressive: Inhibition of Con A-Induced proliferation (IC ₅₀ = $30.8 \mu\text{g mL}^{-1}$); Inhibition of LPS-Induced proliferation (IC ₅₀ = $31.2 \mu\text{g mL}^{-1}$)		
Remisporsine B (169)	Immunosuppressive: Inhibition of Con A-Induced proliferation (IC ₅₀ = $30.1 \mu\text{g mL}^{-1}$); Inhibition of LPS-Induced proliferation (IC ₅₀ = $32.4 \mu\text{g mL}^{-1}$)		

Table 8. Cont.

Name	Activity	Source	Ref.
Paeciloxanthone (68)	Anti-Alzheimer: acetylcholinesterase inhibition (IC ₅₀ = 2.25 µg mL ⁻¹)	<i>Paecilomyces</i> sp. isolated from a mangrove collected in the Taiwan Strait	[40]
Chaetoxanthone A (78)	Antiprotozoal: <i>T. brucei rhodesiense</i> (strain STIB 900) (IC ₅₀ = 4.7 µg mL ⁻¹); <i>T. cruzi</i> (strain Tulahuen C4) (IC ₅₀ ≥ 10 µg mL ⁻¹); <i>L. donovani</i> (strain MHOM-ET-67/L82) (IC ₅₀ = 5.3 µg mL ⁻¹); <i>P. falciparum</i> (IC ₅₀ 3.5 µg mL ⁻¹)		
Chaetoxanthone B (79)	Antiprotozoal: <i>T. brucei rhodesiense</i> (strain STIB 900) (IC ₅₀ = 9.3 µg mL ⁻¹); <i>T. cruzi</i> (strain Tulahuen C4) (IC ₅₀ = 7.1 µg mL ⁻¹); <i>L. donovani</i> (strain MHOM-ET-67/L82) (IC ₅₀ = 3.4 µg mL ⁻¹); <i>P. falciparum</i> (IC ₅₀ = 0.5 µg mL ⁻¹)	<i>Chaetomium</i> sp. isolated from the Greek alga collected at Santorini Island	[41,102,103]
Chaetoxanthone C (80)	Antiprotozoal: <i>T. brucei rhodesiense</i> (strain STIB 900) (IC ₅₀ = 42.6 µg mL ⁻¹); <i>T. cruzi</i> (strain Tulahuen C4) (IC ₅₀ = 1.5 µg mL ⁻¹); <i>L. donovani</i> (strain MHOM-ET-67/L82) (IC ₅₀ = 3.1 µg mL ⁻¹); <i>P. falciparum</i> (IC ₅₀ = 4.0 µg mL ⁻¹)		
Aspergixanthone A (82)	Against aquatic pathogens: <i>V. parahemolyticus</i> (MIC = 25.0 µM); <i>V. anguillarum</i> (MIC = 25.0 µM); <i>V. alginolyticus</i> (MIC = 25.0 µM)	<i>Aspergillus</i> sp. (ZA-01)	[104]
Sterigmatocystin A (110)	Angiogenesis: Increase length of intersomitic vessels of transgenic zebrafish at 1.25 µM	<i>Aspergillus versicolor</i> (15XS43ZD-1) isolated from a sponge collected at Xisha Island	[91]
Aspergixanthone I (114)	Against aquatic pathogens: <i>V. parahemolyticus</i> (MIC = 1.56 µM); <i>V. anguillarum</i> (MIC = 1.56 µM); <i>V. alginolyticus</i> (MIC = 3.12 µM)		
Aspergixanthone J (115)	Against aquatic pathogens: <i>V. parahemolyticus</i> (MIC = 6.25 µM); <i>V. anguillarum</i> (MIC = 25.0 µM); <i>V. alginolyticus</i> (MIC = 25.0 µM)		
Aspergixanthone K (116)	Against aquatic pathogens: <i>V. parahemolyticus</i> (MIC = 3.12 µM); <i>V. anguillarum</i> (MIC = 25.0 µM); <i>V. alginolyticus</i> (MIC = 12.5 µM)	<i>Aspergillus</i> sp. (ZA-01)	[104]
15-Acetyl tajixanthone hydrate (117)	Against aquatic pathogens: <i>V. parahemolyticus</i> (MIC = 12.5 µM); <i>V. anguillarum</i> (MIC = 25.0 µM); <i>V. alginolyticus</i> (MIC = 12.5 µM)		
Tajixanthone hydrate (118)	Against aquatic pathogens: <i>V. parahemolyticus</i> (MIC = 6.25 µM); <i>V. anguillarum</i> (MIC = 6.25 µM); <i>V. alginolyticus</i> (MIC = 12.5 µM)		
16-Chlorotajixanthone (119)	Against aquatic pathogens: <i>V. parahemolyticus</i> (MIC = 25.0 µM); <i>V. anguillarum</i> (MIC = 6.25 µM); <i>V. alginolyticus</i> (MIC = 25.0 µM)		
Isosecosterigmatocystin (169)	Against aquatic pathogens: <i>Ed. ictaluri</i> (IC ₅₀ = 16 µg mL ⁻¹)	<i>Aspergillus nidulans</i> (MA-143) isolated from <i>Rhizophora</i> <i>stylosa</i>	[105]

Con A: Concanavalin A; *Ed. ictaluri*: *Edwardsiella ictaluri*; IC₅₀: Half maximal inhibitory concentration; MIC: Minimum inhibitory concentration, *L. donovani*: *Leishmania donovani*; LPS: Lipopolysaccharide; *T. brucei*: *Trypanosoma brucei*; *T. cruzi*: *Trypanosoma cruzi*; *V. alginolyticus*: *Vibrio alginolyticus*; *V. anguillarum*: *Vibrio anguillarum*; *V. parahemolyticus*: *Vibrio parahemolyticus*.

5. Conclusions

As far as we know, 169 bioactive marine xanthone derivatives were reported in the literature up to 2021. They were isolated from microorganisms, mainly from *Aspergillus* sp., which normally live in an endophytic relationship with microorganisms (e.g., algae, sponge, mangrove, among others).

The chemical space occupied by bioactive marine xanthenes was described through molecular descriptors. For each structural category, the distribution of the MW, Fsp3, number of RB, Log P, TPSA, and Log S values were described and analyzed. The descriptors

were framed accordingly to the NP and drug-likeness concepts. Among the different structural categories of xanthenes, “hydroxanthenes” and “O-heterocyclic” xanthenes are those that better resemble NPs and the ones that better fulfill the drug-likeness criteria. Therefore, hydroxanthenes” and “O-heterocyclic” xanthenes represent the most promising starting point for a hit-to-lead expansion.

In terms of biological activities, a total of 13 different activities were reported for marine xanthenes. The antitumor and antibacterial activities were the most predominant. Potent antitumor marine xanthenes ($IC_{50} < 10 \mu M$) were identified mostly against HeLa (cervical carcinoma), A549 (non-small cell lung carcinoma), HL-60 (acute myeloid leukemia), HCT-116 (colon carcinoma), and MCG-803 (Gastric mucinous adenocarcinoma) cells lines. The most potent antibacterial marine xanthenes ($MIC < 4 \mu g mL^{-1}$) were identified predominantly against Gram-positive bacteria, namely against *S. aureus*, *B. subtilis*, and *E. faecalis*.

Xanthenes isolated from marine and terrestrial organisms share a similar biosynthetic pathway. However, marine-derived xanthenes have not been as exploited as terrestrial-derived xanthenes in traditional drug discovery campaigns. The numerous and relevant bioactive xanthenes isolated from the marine environment could inspire the development of new drugs. The data concerning this review allow us to go deeper in understanding molecular properties, at different levels, of such an important family of marine NP.

Supplementary Materials: The following are available online at <https://www.mdpi.com/article/10.3390/md20010058/s1>, Table S1: Molecular descriptors of the bioactive marine xanthenes, Table S2: NP-likeness and drug-likeness scores of the bioactive marine xanthenes, Table S3: Chemical functional groups present in bioactive marine xanthenes.

Author Contributions: Conceptualization, J.X.S. and C.M.M.A.; writing—original draft preparation, J.X.S., D.R.P.L., A.L.D.; writing—review and editing, C.M.M.A., S.R., M.M.M.P.; project administration, S.R., M.M.M.P. All authors have read and agreed to the published version of the manuscript.

Funding: This research was partially supported by FCT/MCTES—Foundation for Science and Technology from the Minister of Science, Technology and Higher Education and European Regional Development Fund (ERDF) under the projects, co-financed by COMPETE 2020, Portugal 2020, PTDC/SAU-PUB/28736/2017 (POCI-01-0145-FEDER-028736), PTDC/CTA-AMB/0853/2021, and within the scope of UIDB/04423/2020, UID/QUI/5000612019, and UIDP/04423/2020 (Group of Natural Products and Medicinal Chemistry). J.X.S. thanks for the FCT Ph.D. Programs, specifically by the BiotechHealth Program (PD/00016/2012), and for the grants (SFRH/BD/98105/2013 and SFRH/BD/116167/2016). DRPL thanks FCT for her Ph.D. grant (SFRH/BD/140844/2018). Gisela Adriano, Liliana Teixeira, and Sara Cravo for the technical support. Maria Sorokina for kindly providing the NP-likeness scores of NP and SM.

Data Availability Statement: The data presented in this study are available in the article.

Conflicts of Interest: The authors declare no conflict of interest.

References

1. Shang, J.; Hu, B.; Wang, J.; Zhu, F.; Kang, Y.; Li, D.; Sun, H.; Kong, D.-X.; Hou, T. Cheminformatic Insight into the Differences between Terrestrial and Marine Originated Natural Products. *J. Chem. Inf. Model.* **2018**, *58*, 1182–1193. [[CrossRef](#)] [[PubMed](#)]
2. Gerwick, W.H.; Moore, B.S. Lessons from the Past and Charting the Future of Marine Natural Products Drug Discovery and Chemical Biology. *Chem. Biol.* **2012**, *19*, 85–98. [[CrossRef](#)] [[PubMed](#)]
3. Carroll, A.R.; Copp, B.R.; Davis, R.A.; Keyzers, R.A.; Prinsep, M.R. Marine Natural Products. *Nat. Prod. Rep.* **2021**, *38*, 362–413. [[CrossRef](#)] [[PubMed](#)]
4. Loureiro, D.R.P.; Magalhães, Á.F.; Soares, J.X.; Pinto, J.; Azevedo, C.M.G.; Vieira, S.; Henriques, A.; Ferreira, H.; Neves, N.; Bousbaa, H.; et al. Yicathins B and C and Analogues: Total Synthesis, Lipophilicity and Biological Activities. *ChemMedChem* **2020**, *15*, 749–755. [[CrossRef](#)] [[PubMed](#)]
5. Loureiro, D.R.P.; Soares, J.X.; Costa, J.C.; Magalhães, Á.F.; Azevedo, C.M.G.; Pinto, M.M.M.; Afonso, C.M.M. Structures, Activities and Drug-Likeness of Anti-Infective Xanthone Derivatives Isolated from the Marine Environment: A Review. *Molecules* **2019**, *24*, 243. [[CrossRef](#)] [[PubMed](#)]

6. Pinto, M.M.M.; Castanheiro, R.A.P.; Kijjoa, A. Xanthonones from marine-derived microorganisms: Isolation, structure elucidation and biological activities. In *Encyclopedia of Analytical Chemistry*; John Wiley & Sons, Ltd.: Chichester, UK, 2014; pp. 1–21, ISBN 978-0-470-02731-8.
7. Pinto, M.M.M.; Palmeira, A.; Fernandes, C.; Resende, D.I.S.P.; Sousa, E.; Cidade, H.; Tiritan, M.E.; Correia-da-Silva, M.; Cravo, S. From Natural Products to New Synthetic Small Molecules: A Journey through the World of Xanthonones. *Molecules* **2021**, *26*, 431. [[CrossRef](#)]
8. Oprea, T.I.; Gottfries, J. Chemography: The Art of Navigating in Chemical Space. *J. Comb. Chem.* **2001**, *3*, 157–166. [[CrossRef](#)]
9. Lipinski, C.A.; Lombardo, F.; Dominy, B.W.; Feeney, P.J. Experimental and Computational Approaches to Estimate Solubility and Permeability in Drug Discovery and Development Settings. *Adv. Drug Deliv. Rev.* **2001**, *46*, 3–26. [[CrossRef](#)]
10. Veber, D.F.; Johnson, S.R.; Cheng, H.-Y.; Smith, B.R.; Ward, K.W.; Kopple, K.D. Molecular Properties That Influence the Oral Bioavailability of Drug Candidates. *J. Med. Chem.* **2002**, *45*, 2615–2623. [[CrossRef](#)] [[PubMed](#)]
11. Ghose, A.K.; Viswanadhan, V.N.; Wendoloski, J.J. A Knowledge-Based Approach in Designing Combinatorial or Medicinal Chemistry Libraries for Drug Discovery. 1. A Qualitative and Quantitative Characterization of Known Drug Databases. *J. Comb. Chem.* **1999**, *1*, 55–68. [[CrossRef](#)]
12. Egan, W.J.; Merz, K.M.; Baldwin, J.J. Prediction of Drug Absorption Using Multivariate Statistics. *J. Med. Chem.* **2000**, *43*, 3867–3877. [[CrossRef](#)] [[PubMed](#)]
13. Gleeson, M.P. Generation of a Set of Simple, Interpretable ADMET Rules of Thumb. *J. Med. Chem.* **2008**, *51*, 817–834. [[CrossRef](#)] [[PubMed](#)]
14. Bickerton, G.R.; Paolini, G.V.; Besnard, J.; Muresan, S.; Hopkins, A.L. Quantifying the Chemical Beauty of Drugs. *Nat. Chem.* **2012**, *4*, 90–98. [[CrossRef](#)] [[PubMed](#)]
15. Ertl, P.; Roggo, S.; Schuffenhauer, A. Natural Product-Likeness Score and Its Application for Prioritization of Compound Libraries. *J. Chem. Inf. Model.* **2008**, *48*, 68–74. [[CrossRef](#)] [[PubMed](#)]
16. Jayaseelan, K.V.; Moreno, P.; Truszkowski, A.; Ertl, P.; Steinbeck, C. Natural Product-Likeness Score Revisited: An Open-Source, Open-Data Implementation. *BMC Bioinform.* **2012**, *13*, 106. [[CrossRef](#)]
17. Daina, A.; Michielin, O.; Zoete, V. SwissADME: A Free Web Tool to Evaluate Pharmacokinetics, Drug-Likeness and Medicinal Chemistry Friendliness of Small Molecules. *Sci. Rep.* **2017**, *7*, 42717. [[CrossRef](#)] [[PubMed](#)]
18. Matsson, P.; Kihlberg, J. How Big Is Too Big for Cell Permeability? *J. Med. Chem.* **2017**, *60*, 1662–1664. [[CrossRef](#)] [[PubMed](#)]
19. Wei, W.; Cherukupalli, S.; Jing, L.; Liu, X.; Zhan, P. Fsp3: A New Parameter for Drug-Likeness. *Drug Discov.* **2020**, *25*, 1839–1845. [[CrossRef](#)]
20. Hann, M.M.; Keserü, G.M. Finding the Sweet Spot: The Role of Nature and Nurture in Medicinal Chemistry. *Nat. Rev. Drug Discov.* **2012**, *11*, 355–365. [[CrossRef](#)]
21. Caron, G.; Ermondi, G. Molecular Descriptors for Polarity: The Need for Going beyond Polar Surface Area. *Future Med. Chem.* **2016**, *8*, 2013–2016. [[CrossRef](#)] [[PubMed](#)]
22. Li, D.; Edward, H.K.; Guy, T.C. Drug-Like Property Concepts in Pharmaceutical Design. *Curr. Pharm. Des.* **2009**, *15*, 2184–2194. [[CrossRef](#)]
23. Meanwell, N.A. Improving Drug Candidates by Design: A Focus on Physicochemical Properties As a Means of Improving Compound Disposition and Safety. *Chem. Res. Toxicol.* **2011**, *24*, 1420–1456. [[CrossRef](#)] [[PubMed](#)]
24. Sorokina, M.; Steinbeck, C. NaPLoS: A Natural Products Likeness Scorer—Web Application and Database. *J. Cheminformatics* **2019**, *11*, 55. [[CrossRef](#)] [[PubMed](#)]
25. Stratton, C.F.; Newman, D.J.; Tan, D.S. Cheminformatic Comparison of Approved Drugs from Natural Product versus Synthetic Origins. *Bioorg. Med. Chem. Lett.* **2015**, *25*, 4802–4807. [[CrossRef](#)] [[PubMed](#)]
26. Doak, B.C.; Over, B.; Giordanetto, F.; Kihlberg, J. Oral Druggable Space beyond the Rule of 5: Insights from Drugs and Clinical Candidates. *Chem. Biol.* **2014**, *21*, 1115–1142. [[CrossRef](#)] [[PubMed](#)]
27. Ganesan, A. The Impact of Natural Products upon Modern Drug Discovery. *Curr. Opin. Chem. Biol.* **2008**, *12*, 306–317. [[CrossRef](#)] [[PubMed](#)]
28. Yao, Q.F.; Wang, J.E.; Zhang, X.Y.; Nong, X.H.; Xu, X.Y.; Qi, S.H. Cytotoxic Polyketides from the Deep-Sea-Derived Fungus *Engyodontium Album* DFFSCS021. *Mar. Drugs* **2014**, *12*, 5902–5915. [[CrossRef](#)] [[PubMed](#)]
29. Yang, J.X.; Qiu, S.; She, Z.; Lin, Y. A New Xanthone Derivative from the Marine Fungus *Phomopsis* sp. (No. SK7RN3G1). *Chem. Nat. Compd.* **2013**, *49*, 31–33. [[CrossRef](#)]
30. Krick, A.; Kehraus, S.; Gerhäuser, C.; Klimo, K.; Nieger, M.; Maier, A.; Fiebig, H.H.; Atodiresei, I.; Raabe, G.; Fleischhauer, J.; et al. Potential Cancer Chemopreventive in Vitro Activities of Monomeric Xanthone Derivatives from the Marine Algicolous Fungus *Monodictys Putredinis*. *J. Nat. Prod.* **2007**, *70*, 353–360. [[CrossRef](#)]
31. Wang, C.N.; Lu, H.M.; Gao, C.H.; Guo, L.; Zhan, Z.Y.; Wang, J.J.; Liu, Y.H.; Xiang, S.T.; Wang, J.; Luo, X.W. Cytotoxic Benzopyrone and Xanthone Derivatives from a Coral Symbiotic Fungus *Cladosporium Halotolerans* GXIMD 02502. *Nat. Prod. Res.* **2020**, *27*, 1–8. [[CrossRef](#)]
32. Wang, W.Y.; Gao, M.L.; Luo, Z.H.; Liao, Y.Y.; Zhang, B.B.; Ke, W.Q.; Shao, Z.Z.; Li, F.; Chen, J.M. Secondary Metabolites Isolated from the Deep Sea-Derived Fungus *Aspergillus Sydowii* C1-S01-A7. *Nat. Prod. Res.* **2019**, *33*, 3077–3082. [[CrossRef](#)] [[PubMed](#)]
33. Guo, W.Q.; Li, D.; Peng, J.X.; Zhu, T.J.; Gu, Q.Q.; Li, D.H. Penicitols A–C and Penixanacid A from the Mangrove-Derived *Penicillium Chrysogenum* HDN11-24. *J. Nat. Prod.* **2015**, *78*, 306–310. [[CrossRef](#)] [[PubMed](#)]

34. Qin, C.; Lin, X.P.; Lu, X.; Wan, J.T.; Zhou, X.F.; Liao, S.R.; Tu, Z.C.; Xu, S.H.; Liu, Y.H. Sesquiterpenoids and Xanthenes Derivatives Produced by Sponge-Derived Fungus *Stachybotry* sp. HH1 ZSDS1F1-2. *J. Antibiot.* **2015**, *68*, 121–125. [[CrossRef](#)]
35. Yamazaki, H.; Rotinsulu, H.; Kaneko, T.; Murakami, K.; Fujiwara, H.; Ukai, K.; Namikoshi, M. A New Dibenz[b,e]Oxepine Derivative, 1-Hydroxy-10-Methoxy-Dibenz[b,e]Oxepin-6,11-Dione, from a Marine-Derived Fungus, *Beauveria Bassiana* TPU942. *Mar. Drugs* **2012**, *10*, 2691–2697. [[CrossRef](#)]
36. Tao, H.M.; Wei, X.Y.; Lin, X.P.; Zhou, X.F.; Dong, J.D.; Yang, B. Penixanthenes A and B, Two New Xanthone Derivatives from Fungus *Penicillium* sp. SYFz-1 Derived of Mangrove Soil Sample. *Nat. Prod. Res.* **2017**, *31*, 2218–2222. [[CrossRef](#)] [[PubMed](#)]
37. Tian, Y.Q.; Qin, X.C.; Lin, X.P.; Kaliyaperumal, K.; Zhou, X.F.; Liu, J.; Ju, Z.R.; Tu, Z.C.; Liu, Y.H. Sydoxanthone C and Acremolin B Produced by Deep-Sea-Derived Fungus *Aspergillus* sp. SCSIO Ind09F01. *J. Antibiot.* **2015**, *68*, 703–706. [[CrossRef](#)]
38. Elnaggar, M.S.; Ebada, S.S.; Ashour, M.L.; Ebrahim, W.; Muller, W.E.G.; Mandi, A.; Kurtan, T.; Singab, A.; Lin, W.H.; Liu, Z.; et al. Xanthenes and Sesquiterpene Derivatives from a Marine-Derived Fungus *Scopulariopsis* sp. *Tetrahedron* **2016**, *72*, 2411–2419. [[CrossRef](#)]
39. Li, F.; Guo, W.Q.; Che, Q.; Zhu, T.J.; Gu, Q.Q.; Li, D.H. Versicones E-H and Arugosin K Produced by the Mangrove-Derived Fungus *Aspergillus Versicolor* HDN11-84. *J. Antibiot.* **2017**, *70*, 174–178. [[CrossRef](#)] [[PubMed](#)]
40. Wen, L.; Lin, Y.C.; She, Z.G.; Du, D.S.; Chan, W.L.; Zheng, Z.H. Paeciloxanthone, a New Cytotoxic Xanthone from the Marine Mangrove Fungus *Paecilomyces* sp. (Tree1-7). *J. Asian Nat. Prod. Res.* **2008**, *10*, 133–137. [[CrossRef](#)] [[PubMed](#)]
41. Pontius, A.; Krick, A.; Kehraus, S.; Brun, R.; König, G.M. Antiprotozoal Activities of Heterocyclic-Substituted Xanthenes from the Marine-Derived Fungus *Chaetomium* sp. *J. Nat. Prod.* **2008**, *71*, 1579–1584. [[CrossRef](#)]
42. Zhu, F.; Lin, Y.C. Three Xanthenes from a Marine-Derived Mangrove Endophytic Fungus. *Chem. Nat. Compd.* **2007**, *43*, 132–135. [[CrossRef](#)]
43. Lee, Y.M.; Li, H.; Hong, J.; Cho, H.Y.; Bae, K.S.; Kim, M.A.; Kim, D.K.; Jung, J.H. Bioactive Metabolites from the Sponge-Derived Fungus *Aspergillus Versicolor*. *Arch. Pharm. Res.* **2010**, *33*, 231–235. [[CrossRef](#)] [[PubMed](#)]
44. Li, J.L.; Jiang, X.; Liu, X.P.; He, C.W.; Di, Y.X.; Lu, S.J.; Huang, H.L.; Lin, B.; Wang, D.; Fan, B.Y. Antibacterial Anthraquinone Dimers from Marine Derived Fungus *Aspergillus* sp. *Fitoterapia* **2019**, *133*, 1–4. [[CrossRef](#)] [[PubMed](#)]
45. Zhu, A.; Yang, M.Y.; Zhang, Y.H.; Shao, C.L.; Wang, C.Y.; Hu, L.D.; Cao, F.; Zhu, H.J. Absolute Configurations of 14,15-Hydroxylated Prenylxanthenes from a Marine-Derived *Aspergillus* sp. Fungus by Chiroptical Methods. *Sci. Rep.* **2018**, *8*, 10621. [[CrossRef](#)] [[PubMed](#)]
46. Cai, S.X.; Zhu, T.J.; Du, L.; Zhao, B.Y.; Li, D.H.; Gu, Q.Q. Sterigmatocystins from the Deep-Sea-Derived Fungus *Aspergillus Versicolor*. *J. Antibiot.* **2011**, *64*, 193–196. [[CrossRef](#)] [[PubMed](#)]
47. Liu, F.A.; Lin, X.; Zhou, X.; Chen, M.; Huang, X.; Yang, B.; Tao, H. Xanthenes and Quinolones Derivatives Produced by the Deep-Sea-Derived Fungus *Penicillium* sp. SCSIO Ind16F01. *Molecules* **2017**, *22*, 1999. [[CrossRef](#)]
48. Ding, B.; Yuan, J.; Huang, X.S.; Wen, W.T.; Zhu, X.; Liu, Y.Y.; Li, H.X.; Lu, Y.J.; He, L.; Tan, H.M.; et al. New Dimeric Members of the Phomoxanthone Family: Phomolactonexanthenes A, B and Deacetylphomoxanthone C Isolated from the Fungus *Phomopsis* sp. *Mar. Drugs* **2013**, *11*, 4961–4972. [[CrossRef](#)]
49. Tang, R.; Kimishima, A.; Setiawan, A.; Arai, M. Secalonic Acid D as a Selective Cytotoxic Substance on the Cancer Cells Adapted to Nutrient Starvation. *J. Nat. Med.* **2020**, *74*, 495–500. [[CrossRef](#)]
50. Zhen, X.; Gong, T.; Wen, Y.H.; Yan, D.J.; Chen, J.J.; Zhu, P. A Chrysoxanthenes A-C, Three New Xanthone-Chromanone Heterodimers from Sponge-Associated *Penicillium* Chrysozogenum HLS111 Treated with Histone Deacetylase Inhibitor. *Mar. Drugs* **2018**, *16*, 357. [[CrossRef](#)]
51. Chen, L.; Li, Y.P.; Li, X.X.; Lu, Z.H.; Zheng, Q.H.; Liu, Q.Y. Isolation of 4,4'-Bond Secalonic Acid D from the Marine-Derived Fungus *Penicillium Oxalicum* with Inhibitory Property against Hepatocellular Carcinoma. *J. Antibiot.* **2019**, *72*, 34–44. [[CrossRef](#)]
52. Wu, G.W.; Qi, X.; Mo, X.M.; Yu, G.H.; Wang, Q.; Zhu, T.J.; Gu, Q.Q.; Liu, M.; Li, J.; Li, D.H. Structure-Based Discovery of Cytotoxic Dimeric Tetrahydroxanthenes as Potential Topoisomerase I Inhibitors from a Marine-Derived Fungus. *Eur. J. Med. Chem.* **2018**, *148*, 268–278. [[CrossRef](#)]
53. Liu, L.L.; He, L.S.; Xu, Y.; Han, Z.; Li, Y.X.; Zhong, J.L.; Guo, X.R.; Zhang, X.X.; Ko, K.M.; Qian, P.Y. Caspase-3-Dependent Apoptosis of Citreamicin ϵ -Induced HeLa Cells Is Associated with Reactive Oxygen Species Generation. *Chem. Res. Toxicol.* **2013**, *26*, 1055–1063. [[CrossRef](#)]
54. Yeon, J.T.; Kim, H.; Kim, K.J.; Lee, J.; Won, D.H.; Nam, S.J.; Kim, S.H.; Kang, H.; Son, Y.J. Acredinone C and the Effect of Acredinones on Osteoclastogenic and Osteoblastogenic Activity. *J. Nat. Prod.* **2016**, *79*, 1730–1736. [[CrossRef](#)] [[PubMed](#)]
55. Pavão, G.B.; Venâncio, V.P.; de Oliveira, A.L.L.; Hernandes, L.C.; Almeida, M.R.; Antunes, L.M.G.; Debonsi, H.M. Differential Genotoxicity and Cytotoxicity of Phomoxanthone A Isolated from the Fungus *Phomopsis Longicolla* in HL60 Cells and Peripheral Blood Lymphocytes. *Toxicol. Vitro* **2016**, *37*, 211–217. [[CrossRef](#)] [[PubMed](#)]
56. Ueda, J.Y.; Takagi, M.; Shin-Ya, K. New Xanthoquinodin-like Compounds, JBIR-97,-98 and-99, Obtained from Marine Sponge-Derived Fungus *Tritirachium* sp. SpB081112MEf2. *J. Antibiot.* **2010**, *63*, 615–618. [[CrossRef](#)] [[PubMed](#)]
57. Moon, K.; Chung, B.; Shin, Y.; Rheingold, A.L.; Moore, C.E.; Park, S.J.; Park, S.; Lee, S.K.; Oh, K.B.; Shin, J.; et al. Pentacyclic Antibiotics from a Tidal Mud Flat-Derived Actinomycete. *J. Nat. Prod.* **2015**, *78*, 524–529. [[CrossRef](#)] [[PubMed](#)]
58. Koyanagi, Y.; Kawahara, T.; Hitora, Y.; Tsukamoto, S. Ukixanthomycin A: A Hexacyclic Xanthone from the Mudflat-Derived Actinomycete *Streptomyces* sp. *Heterocycles* **2020**, *100*, 1686–1693. [[CrossRef](#)]

59. Li, H.L.; Li, X.M.; Liu, H.; Meng, L.H.; Wang, B.G. Two New Diphenylketones and a New Xanthone from *Talaromyces Islandicus* EN-501, an Endophytic Fungus Derived from the Marine Red Alga *Laurencia Okamurai*. *Mar. Drugs* **2016**, *14*, 223. [[CrossRef](#)] [[PubMed](#)]
60. Liu, F.; Cai, X.L.; Yang, H.; Xia, X.K.; Guo, Z.Y.; Yuan, J.; Li, M.F.; She, Z.G.; Lin, Y.C. The Bioactive Metabolites of the Mangrove Endophytic Fungus *Talaromyces* sp. ZH-154 Isolated from *Kandelia Candel* (L.) Druce. *Planta Med.* **2010**, *76*, 185–189. [[CrossRef](#)]
61. Sun, R.R.; Miao, F.P.; Zhang, J.; Wang, G.; Yin, X.L.; Ji, N.Y. Three New Xanthone Derivatives from an Algicolous Isolate of *Aspergillus Wentii*. *Magn. Reson. Chem.* **2013**, *51*, 65–68. [[CrossRef](#)]
62. Wang, J.H.; Ding, W.J.; Wang, R.M.; Du, Y.P.; Liu, H.L.; Kong, X.H.; Li, C.Y. Identification and Bioactivity of Compounds from the Mangrove Endophytic Fungus *Alternaria* sp. *Mar. Drugs* **2015**, *13*, 4492–4504. [[CrossRef](#)] [[PubMed](#)]
63. Ji, Y.B.; Chen, W.J.; Shan, T.Z.; Sun, B.Y.; Yan, P.C.; Jiang, W. Antibacterial Diphenyl Ether, Benzophenone and Xanthone Derivatives from *Aspergillus Flavipes*. *Chem. Biodivers.* **2020**, *17*, 5. [[CrossRef](#)] [[PubMed](#)]
64. Song, Z.; Gao, J.; Hu, J.; He, H.; Huang, P.; Zhang, L.; Song, F. One New Xanthenone from the Marine-Derived Fungus *Aspergillus Versicolor* MF160003. *Nat. Prod. Res.* **2020**, *34*, 2907–2912. [[CrossRef](#)]
65. Khoshbakht, M.; Thanaussavate, B.; Zhu, C.X.; Cao, Y.; Zakharov, L.N.; Loesgen, S.; Blakemore, P.R. Total Synthesis of Chalaniline B: An Antibiotic Aminoxanthone from Vorinostat-Treated Fungus *Chalara* sp. 6661. *J. Org. Chem.* **2021**, *86*, 7773–7780. [[CrossRef](#)]
66. Zhang, W.; Krohn, K.; Zia-Ullah, F.U.; Pescitelli, G.; Di Bari, L.; Antus, S.; Kurtán, T.; Rheinheimer, J.; Draeger, S.; Schulz, B. New Mono- and Dimeric Members of the Secalonic Acid Family: Blennolides A–G Isolated from the Fungus *Blennoria* sp. *Chem. Eur. J.* **2008**, *14*, 4913–4923. [[CrossRef](#)]
67. Song, F.H.; Ren, B.; Chen, C.X.; Yu, K.; Liu, X.R.; Zhang, Y.H.; Yang, N.; He, H.T.; Liu, X.T.; Dai, H.Q.; et al. Three New Sterigmatocystin Analogues from Marine-Derived Fungus *Aspergillus Versicolor* MF359. *Appl. Microbiol. Biotechnol.* **2014**, *98*, 3753–3758. [[CrossRef](#)] [[PubMed](#)]
68. Fredimoses, M.; Zhou, X.F.; Ai, W.; Tian, X.P.; Yang, B.; Lin, X.P.; Liu, J.; Liu, Y.H. Emerixanthone E, a New Xanthone Derivative from Deep Sea Fungus *Emericella* sp. SCSIO 05240. *Nat. Prod. Res.* **2019**, *33*, 2088–2094. [[CrossRef](#)] [[PubMed](#)]
69. Fredimoses, M.; Zhou, X.F.; Lin, X.P.; Tian, X.P.; Ai, W.; Wang, J.F.; Liao, S.R.; Liu, J.; Yang, B.; Yang, X.W.; et al. New Prenylxanthenones from the Deep-Sea Derived Fungus *Emericella* sp. SCSIO 05240. *Mar. Drugs* **2014**, *12*, 3190–3202. [[CrossRef](#)] [[PubMed](#)]
70. Malmstrøm, J.; Christophersen, C.; Barrero, A.F.; Enrique Oltra, J.; Justicia, J.; Rosales, A. Bioactive Metabolites from a Marine-Derived Strain of the Fungus *Emericella Variicolor*. *J. Nat. Prod.* **2002**, *65*, 364–367. [[CrossRef](#)] [[PubMed](#)]
71. Tian, Y.Q.; Lin, S.T.; Kumaravel, K.; Zhou, H.; Wang, S.Y.; Liu, Y.H. Polyketide-Derived Metabolites from the Sponge-Derived Fungus *Aspergillus* sp. F40. *Phytochem. Lett.* **2018**, *27*, 74–77. [[CrossRef](#)]
72. Erbert, C.; Lopes, A.A.; Yokoya, N.S.; Furtado, N.; Conti, R.; Pupo, M.T.; Lopes, J.L.C.; Debonis, H.M. Antibacterial Compound from the Endophytic Fungus *Phomopsis Longicolla* Isolated from the Tropical Red Seaweed *Bostrychia Radicans*. *Bot. Mar.* **2012**, *55*, 435–440. [[CrossRef](#)]
73. Wang, Y.; Lin, X.P.; Ju, Z.R.; Liao, X.J.; Huang, X.J.; Zhang, C.; Zhao, B.X.; Xu, S.H. Aspergichromones A and B, Two New Polyketides from the Marine Sponge-Associated Fungus *Aspergillus* sp. SCSIO XWS03F03. *J. Asian Nat. Prod. Res.* **2017**, *19*, 684–690. [[CrossRef](#)] [[PubMed](#)]
74. Bao, J.; Sun, Y.L.; Zhang, X.Y.; Han, Z.; Gao, H.C.; He, F.; Qian, P.Y.; Qi, S.H. Antifouling and Antibacterial Polyketides from Marine Gorgonian Coral-Associated Fungus *Penicillium* sp. SCSGAF 0023. *J. Antibiot.* **2013**, *66*, 219–223. [[CrossRef](#)] [[PubMed](#)]
75. Wu, B.; Wiese, J.; Wenzel-Storjohann, A.; Malien, S.; Schmaljohann, R.; Imhoff, J.F. Engyodontochones, Antibiotic Polyketides from the Marine Fungus *Engyodontium Album* Strain LF069. *Chem. Eur. J.* **2016**, *22*, 7452–7462. [[CrossRef](#)] [[PubMed](#)]
76. Eltamany, E.E.; Abdelmohsen, U.R.; Ibrahim, A.K.; Hassanean, H.A.; Hentschel, U.; Ahmed, S.A. New Antibacterial Xanthone from the Marine Sponge-Derived *Micrococcus* sp. EG45. *Bioorg. Med. Chem. Lett.* **2014**, *24*, 4939–4942. [[CrossRef](#)]
77. Liu, L.L.; Xu, Y.; Han, Z.; Li, Y.X.; Lu, L.; Lai, P.Y.; Zhong, J.L.; Guo, X.R.; Zhang, X.X.; Qian, P.Y. Four New Antibacterial Xanthenes from the Marine-Derived Actinomycetes *Streptomyces Caelestis*. *Mar. Drugs* **2012**, *10*, 2571–2583. [[CrossRef](#)]
78. Malet-Cascón, L.; Romero, F.; Espliego-Vázquez, F.; Grávalos, D.; Fernández-Puentes, J.L. IB-00208, a New Cytotoxic Polycyclic Xanthone Produced by a Marine-Derived Actinomadura. I. Isolation of the Strain, Taxonomy and Biological Activities. *J. Antibiot.* **2003**, *56*, 219–225. [[CrossRef](#)] [[PubMed](#)]
79. Peoples, A.J.; Zhang, Q.B.; Millett, W.P.; Rothfeder, M.T.; Peseatore, B.C.; Madden, A.A.; Ling, L.L.; Moore, C.M. Neocitreamicins I and II, Novel Antibiotics with Activity against Methicillin-Resistant *Staphylococcus Aureus* and Vancomycin-Resistant Enterococci. *J. Antibiot.* **2008**, *61*, 457–463. [[CrossRef](#)]
80. Maiese, W.M.; Lechevalier, M.P.; Lechevalier, H.A.; Korshalla, J.; Goodman, J.; Wildey, M.J.; Kuck, N.; Greenstein, M. LL-E19085 Alpha, a Novel Antibiotic from *Micromonospora Citrea*: Taxonomy, Fermentation and Biological Activity. *J. Antibiot.* **1989**, *42*, 846–851. [[CrossRef](#)]
81. Abdel-Lateff, A.; Klemke, C.; König, G.M.; Wright, A.D. Two New Xanthone Derivatives from the Algicolous Marine Fungus *Wardomyces Anomalus*. *J. Nat. Prod.* **2003**, *66*, 706–708. [[CrossRef](#)]
82. Shao, C.; Wang, C.; Wei, M.; Gu, Y.; Xia, X.; She, Z.; Lin, Y. Structure Elucidation of Two New Xanthone Derivatives from the Marine Fungus *Penicillium* sp. (ZZF 32#) from the South China Sea. *Magn. Reson. Chem.* **2008**, *46*, 1066–1069. [[CrossRef](#)]

83. Wang, X.; Mao, Z.G.; Song, B.B.; Chen, C.H.; Xiao, W.W.; Hu, B.; Wang, J.W.; Jiang, X.B.; Zhu, Y.H.; Wang, H.J. Advances in the Study of the Structures and Bioactivities of Metabolites Isolated from Mangrove-Derived Fungi in the South China Sea. *Mar. Drugs* **2013**, *11*, 3601–3616. [[CrossRef](#)]
84. Höller, U.; König, G.M.; Wright, A.D. A New Tyrosine Kinase Inhibitor from a Marine Isolate of *Ulocladium Botrytis* and New Metabolites from the Marine Fungi *Asteromyces Cruciatum* and *Varicosporina Ramulosa*. *Eur. J. Org. Chem.* **1999**, 2949–2955. [[CrossRef](#)]
85. Li, C.Y.; Zhang, J.; Shao, C.L.; Ding, W.J.; She, Z.G.; Lin, Y.C. A New Xanthone Derivative from the Co-Culture Broth of Two Marine Fungi (Strain No. E33 and K38). *Chem. Nat. Compd.* **2011**, *47*, 382–384. [[CrossRef](#)]
86. Marmann, A.; Aly, A.H.; Lin, W.H.; Wang, B.G.; Proksch, P. Co-Cultivation—A Powerful Emerging Tool for Enhancing the Chemical Diversity of Microorganisms. *Mar. Drugs* **2014**, *12*, 1043–1065. [[CrossRef](#)] [[PubMed](#)]
87. Wang, J.F.; He, W.J.; Huang, X.L.; Tian, X.P.; Liao, S.R.; Yang, B.; Wang, F.Z.; Zhou, X.J.; Liu, Y.H. Antifungal New Oxepine-Containing Alkaloids and Xanthenes from the Deep-Sea-Derived Fungus *Aspergillus Versicolor* SCSIO 05879. *J. Agric. Food Chem.* **2016**, *64*, 2910–2916. [[CrossRef](#)] [[PubMed](#)]
88. Luo, X.W.; Yang, J.; Chen, F.M.; Lin, X.P.; Chen, C.M.; Zhou, X.F.; Liu, S.W.; Liu, Y.H. Structurally Diverse Polyketides From the Mangrove-Derived Fungus *Diaporthe* Sp SCSIO 41011 With Their Anti-Influenza A Virus Activities. *Front. Chem.* **2018**, *6*, 10. [[CrossRef](#)]
89. Kang, H.H.; Zhang, H.B.; Zhong, M.J.; Ma, L.Y.; Liu, D.S.; Liu, W.Z.; Ren, H. Potential Antiviral Xanthenes from a Coastal Saline Soil Fungus *Aspergillus Iizukae*. *Mar. Drugs* **2018**, *16*, 449. [[CrossRef](#)] [[PubMed](#)]
90. Liu, N.Z.; Peng, S.; Yang, J.; Cong, Z.W.; Lin, X.P.; Liao, S.R.; Yang, B.; Zhou, X.F.; Zhou, X.J.; Liu, Y.H.; et al. Structurally Diverse Sesquiterpenoids and Polyketides from a Sponge-Associated Fungus *Aspergillus Sydowii* SCSIO41301. *Fitoterapia* **2019**, *135*, 27–32. [[CrossRef](#)] [[PubMed](#)]
91. Han, X.; Tang, X.L.; Luo, X.C.; Sun, C.X.; Liu, K.C.; Zhang, Y.; Li, P.L.; Li, G.Q. Isolation and Identification of Three New Sterigmatocystin Derivatives from the Fungus *Aspergillus Versicolor* Guided by Molecular Networking Approach. *Chem. Biodivers.* **2020**, *17*, 8. [[CrossRef](#)] [[PubMed](#)]
92. Wu, Z.J.; Ouyang, M.A.; Tan, Q.W. New Asperxanthone and Asperbiphenyl from the Marine Fungus *Aspergillus* sp. *Pest Manag. Sci.* **2009**, *65*, 60–65. [[CrossRef](#)] [[PubMed](#)]
93. Tan, S.; Yang, B.; Liu, J.; Xun, T.; Liu, Y.; Zhou, X. Penicillixanthone A, a Marine-Derived Dual-Coreceptor Antagonist as Anti-HIV-1 Agent. *Nat. Prod. Res.* **2019**, *33*, 1467–1471. [[CrossRef](#)]
94. Wang, J.F.; Zhou, L.M.; Chen, S.T.; Yang, B.; Liao, S.R.; Kong, F.D.; Lin, X.P.; Wang, F.Z.; Zhou, X.F.; Liu, Y.H. New Chlorinated Diphenyl Ethers and Xanthenes from a Deep-Sea-Derived Fungus *Penicillium Chrysogenum* SCSIO 41001. *Fitoterapia* **2018**, *125*, 49–54. [[CrossRef](#)] [[PubMed](#)]
95. Gan, Q.; Lin, C.Y.; Lu, C.J.; Chang, Y.M.; Che, Q.; Zhang, G.J.; Zhu, T.J.; Gu, Q.Q.; Wu, Z.Q.; Li, M.Y.; et al. Staprexanthenes, Xanthone-Type Stimulators of Pancreatic Beta-Cell Proliferation from a Mangrove Endophytic Fungus. *J. Nat. Prod.* **2020**, *83*, 2996–3003. [[CrossRef](#)] [[PubMed](#)]
96. Liang, X.; Huang, Z.H.; Ma, X.; Zheng, Z.H.; Zhang, X.X.; Lu, X.H.; Qi, S.H. Mycotoxins as Inhibitors of Protein Tyrosine Phosphatases from the Deep-Sea-Derived Fungus *Aspergillus Puniceus* SCSIO Z021. *Bioorganic Chem.* **2021**, *107*, 104571. [[CrossRef](#)] [[PubMed](#)]
97. Bao, J.; He, F.; Yu, J.H.; Zhai, H.J.; Cheng, Z.Q.; Jiang, C.S.; Zhang, Y.Y.; Zhang, Y.; Zhang, X.Y.; Chen, G.Y.; et al. New Chromones from a Marine-Derived Fungus, *Arthrinium* sp., and Their Biological Activity. *Molecules* **2018**, *23*, 1982. [[CrossRef](#)] [[PubMed](#)]
98. Wu, Z.H.; Liu, D.; Xu, Y.; Chen, J.L.; Lin, W.H. Antioxidant Xanthenes and Anthraquinones Isolated from a Marine-Derived Fungus *Aspergillus Versicolor*. *Chin. J. Nat. Med.* **2018**, *16*, 219–224. [[CrossRef](#)]
99. Du, X.W.; Liu, D.; Huang, J.; Zhang, C.J.; Proksch, P.; Lin, W.H. Polyketide Derivatives from the Sponge Associated Fungus *Aspergillus Europaeus* with Antioxidant and NO Inhibitory Activities. *Fitoterapia* **2018**, *130*, 190–197. [[CrossRef](#)]
100. Wang, J.F.; Xu, F.Q.; Wang, Z.; Lu, X.; Wan, J.T.; Yang, B.; Zhou, X.F.; Zhang, T.Y.; Tu, Z.C.; Liu, Y.H. A New Naphthalene Glycoside from the Sponge-Derived Fungus *Arthrinium* sp. ZSDS1-F3. *Nat. Prod. Res.* **2014**, *28*, 1070–1074. [[CrossRef](#)]
101. Liu, H.J.; Chen, S.H.; Liu, W.Y.; Liu, Y.Y.; Huang, X.S.; She, Z.G. Polyketides with Immunosuppressive Activities from Mangrove Endophytic Fungus *Penicillium* sp. ZJ-SY2. *Mar. Drugs* **2016**, *14*, 217. [[CrossRef](#)]
102. Yang, B.; Huang, J.X.; Zhou, X.F.; Lin, X.P.; Liu, J.; Liao, S.R.; Wang, J.F.; Liu, F.A.; Tao, H.M.; Liu, Y.H. The Fungal Metabolites with Potential Antiplasmodial Activity. *Curr. Med. Chem.* **2018**, *25*, 3796–3825. [[CrossRef](#)] [[PubMed](#)]
103. Tempone, A.G.; de Oliveira, C.M.; Berlinck, R.G.S. Current Approaches to Discover Marine Antileishmanial Natural Products. *Planta Med.* **2011**, *77*, 572–585. [[CrossRef](#)] [[PubMed](#)]
104. Zhu, A.; Zhang, X.W.; Zhang, M.; Li, W.; Ma, Z.Y.; Zhu, H.J.; Cao, F. Aspergixanthenes I–K, New Anti-Vibrio Prenylxanthenes from the Marine-Derived Fungus *Aspergillus* sp. ZA-01. *Mar. Drugs* **2018**, *16*, 312. [[CrossRef](#)] [[PubMed](#)]
105. Yang, S.Q.; Li, X.M.; Xu, G.M.; Li, X.; An, C.Y.; Wang, B.G. Antibacterial Anthraquinone Derivatives Isolated from a Mangrove-Derived Endophytic Fungus *Aspergillus Nidulans* by Ethanol Stress Strategy. *J. Antibiot.* **2018**, *71*, 778–784. [[CrossRef](#)] [[PubMed](#)]